Introducing standardized field methods for fracture-focused surface processes research

Martha Cary Eppes[1], Alex Rinehart[2], Jennifer Aldred[3], Samantha Berberich[1], Maxwell P. Dahlquist[4], Sarah G. Evans[5], Russell Keanini[6], Stephen E. Laubach[7], Faye Moser[1], Mehdi Morovati[6], Steven Porson[1], Monica Rasmussen[1], Uri Shaanan[8]

[1] Department of Geography & Earth Sciences, University of North Carolina at Charlotte, Charlotte, NC 28223, USA

[2] Department of Earth and Environmental Sciences, New Mexico Institute of Mining and Technology, Socorro, NM, 87801, USA

[3] New Mexico Highlands University, Las Vegas, NM, USA

[4] Department of Geology, University of the South, Sewanee, TN 37383, USA

[5] Department of Geological and Environmental Sciences, Appalachian State University, Boone, NC, 28608, USA

[6] Department of Mechanical Engineering and Engineering Science, University of North Carolina at Charlotte, Charlotte, NC 28223, USA

[7] Jackson School of Geosciences, The University of Texas at Austin, Austin, TX 78714

[8] Geological Survey of Israel, Jerusalem 9692100, Israel

Correspondence to: meppes@charlotte.edu

Abstract. Rock fractures are a key contributor to a broad array of Earth surface processes due to their direct control on rock strength as well as rock porosity and permeability. However, to date, there has been no standardization for the quantification of rock fractures in surface processes research. In this work, the case is made for standardization within fracture-focused research, and prior work is reviewed to identify various key datasets and methodologies. Then, a suite of standardized methods is presented as a starting 'baseline' for fracture-based research in surface processes studies. These methods have been shown in preexisting work from structural geology, geotechnical engineering, and surface processes disciplines to comprise best practices for the characterization for fractures in clasts and outcrops. This practical, accessible, and detailed guide can be readily employed across all fracture-focused weathering and geomorphology applications. The wide adoption of a baseline of data collected using the same methods will enable comparison and compilation of datasets among studies globally and will ultimately lead to a better understanding of the links and feedbacks between rock fracture and landscape evolution.

Short Summary. All rocks have fractures (cracks) that can influence virtually every process acting on Earth's surface where humans live. Yet, scientists have not standardized their methods for collecting fracture data. Here we draw on past work across geo-disciplines and propose a list of baseline data for fracture-focused surface processes research. We detail its rationale and the methods for collecting it. We hope its wide adoption will improve future methods and knowledge of rock fracture overall.

1 Introduction

Rock fracture in surface and near-surface environments plays a key role in virtually all Earth surface processes. Fractures comprise faults and opening-mode fractures; both coming in a wide range of sizes. The focus here, however, is on opening-mode fractures. The propagation of opening-mode fractures universally occurs at or near the surface of Earth (e.g., within ~500 m - Moon et al., 2020), on other terrestrial bodies (Molaro et al., 2020), and at depth in the crust (e.g., Laubach et al., 2019). It epitomizes mechanical weathering and the development of 'critical zone architecture', i.e., the evolving porosity, permeability, and strength of near-surface rock (e.g., Riebe et al., 2021). For clarity and consistency herein, the use of the term fracture is limited to refer to any *open,* high-length-to-aperture-ratio discontinuity in rock, regardless of its origin, scale, or location (e.g. within a clast, or within shallow or deep bedrock), acknowledging that veins (partly to completely mineral filled fractures) or dikes (filled with secondary minerals) are also termed 'fractures' in many contexts. The term 'crack' is avoided because the wide-ranging semantics of that term can cause confusion when employed in interdisciplinary work across rock mechanics, structural geology, and geomorphology.

Fracture characteristics (e.g., size, number, connectivity, orientation) exert enormous influence on both rock mechanical properties (e.g., Ayatollahi and Akbardoost, 2014) and rock hydrological properties (e.g., Leone et al., 2020; Snowdon et al., 2021). Fractures therefore influence a wide array of natural and anthropogenic landscape features and processes including channel incision (e.g., Shobe et al., 2017), sediment size and production (Sousa, 2010; Sklar et al., 2017), hillslope erosion (e.g., DiBiase et al., 2018; Neely et al., 2019), built environment degradation (e.g., Hatır, 2020), landslide and rockfall hazards (e.g., Collins and Stock, 2016), groundwater and surface water processes (e.g., Maffucci et al., 2015; Wohl, 2008), and vegetation distribution (e.g., Aich and Gross, 2008). Additionally, the resultant physical properties of fracture-produced sediment (i.e., clast size distribution, mass, porosity, etc.) control both hillslope and stream processes (e.g., Chilton and Spotila, 2020; Glade et al., 2019).

53 With fractures clearly central to so many surface processes, as well as to non-academic concerns such as hazard and infrastructure

54 degradation, it is crucial to understand the factors that control surface and near-surface rock fracture attributes, and rock fracturing

55 rates and processes. To fully do so requires a large body of data quantifying fracture-related characteristics and phenomena in a

56 variety of subaerial environments; however, to date, no standard field methods have been widely adopted to quantify fractures in

57 the modern surface processes realm. Consequently, data collected across studies cannot be readily compared or coalesced. The

58 purpose of this paper is to define an initial set of such standards with the anticipation that the methods will evolve as new

59 understanding, needs and applications ariseWe develop these proposed standards by combining prior fracture methodologies from

60 other geoscience disciplines with those that have been developed, tested and refined through more than 20 years of field-based

61 fracture observations for surface processes-related research (e.g., Aldred et al., 2015; Eppes and Griffing, 2010; Eppes et al., 2018;

62 Eppes et al., 2010; Mcfadden et al., 2005; Moser, 2017; Shobe et al., 2017; Weiserbs, 2017).

63

64 Building on past work, this paper defines the benefits of establishing a standard procedure for fracture-focused surface processes

65 field research, describing how presented methods outperform other approaches. We then provide a short review of motivating

66 existing approaches derived primarily from engineering and structural geology disciplines. Finally, we describe a set of methods

67 that is proposed as a starting point for surface processes researchers so that a larger community of teams can begin to cross-pollinate

68 their observations. When no other standard practice is evident in existing literature, we have suggested rules of thumb that are

69 based on our experience during fieldwork for past published works (e.g. Eppes and McFadden, 2010; Aldred et al., 2016; Ortega

70 et al., 2006). We explicitly note when such practices are presented, and our rationale thereof. The overall scope herein is limited

71 to in-person field observations on sub-aerially exposed rock, i.e., fractures that can be observed with the naked eye or basic hand

72 lens. Measurements of smaller fractures (e.g., those visible with microscopy) or of buried fractures (e.g., those visualized in

73 boreholes or with indirect geophysical methods) are not directly described here. We also note that methods for fracture detection

74 using automated analyses of remote data such as LiDAR, drone photography, structure-from-motion, or 3D modeling are not

75 described herein, but provide motivation for this work (Sect. 1.2).

76

77 In sum, the overall aim of this paper is to build: 1) a motivation for standardization based on existing published work across

78 disciplines 2) a set of guiding principles applicable to all surface processes research involving rock fractures; 3) a list of fracture

79 and rock data measurements that constitute "basic" field-based metrics; and 4) practical methods that comprise best practices for

80 collection of these data. Unless otherwise specified, all methods may be applied to loose clasts or to outcrops. Also provided are

81 some suggestions for data analyses and a demonstration of a real case example of how the proposed methods lead to reproducible

82 results across users. By providing this compendium of fracture-focused field methods, the hope is to accelerate understanding of

83 how a most basic feature of all rock – its open fractures – contributes to the processes and evolution of Earth's surface and critical

84 zone.

85 **1.1 The value of a standardized approach**

86 Particularly within the fields of geomorphology and weathering sciences, no common suite of data, methods, or terminology has

87 been defined or described that comprises an analysis of fractures. Although fracture characterization field methods exist in the

88 context of structural geology and aquifer and reservoir characterization (e.g., Watkins et al., 2015; Wu and Pollard, 1995; Zeeb et

89 al., 2013; Laubach et al., 2018), they diverge significantly in their approaches because they were largely developed for the specific

90 application of each unique study or field of study. Furthermore, the terminology and methodologies used to describe natural

91 fractures across this existing research tend to be applicable to what is typically envisioned as deep-seated processes including

92 tectonic loading and pore pressure elevation (e.g., Schultz, 2019). Numerous published works fail to provide clear criteria for

93 categorizing fractures, or even for choosing which fractures to measure. The choices, of course, depend on the objectives of the

94 study. This lack of consistency severely limits the ability of the geomorphic community to reproduce methods, or to combine,

95 compare, or interpret different fracture datasets.

96

97 The development of consistent methods undergirds most quantitative Earth sciences. For example, the fields of sedimentology and

98 soil science have clear, standardized methods to acquire what constitutes the "basic" data for their observations. Sedimentologists

99 have long shared common metrics and methods for quantifying grain size, sorting, rounding, and stratigraphic records (e.g.,

100 Krumbein, 1943). Similarly, soil scientists share common methods, metrics, and nomenclature for describing soil profiles and

101 horizons (e.g., Birkeland, 1999 Appendix A; Soil Survey Staff, 1999). The realization of the need for standard methods has also

102 remained constant in laboratory-based rock mechanics over the last several decades, driving the American Society for Testing and

103 Materials (ASTM) and International Society for Rock Mechanics (ISMR) to publish ongoing standards and methods papers (e.g.,

104 Ulusay and Hudson, 2007; Ulusay, 2015).

105

106 Standards like those mentioned above exist because workers have long recognized and reaped their benefits. Standardized methods

107 can frequently lead to major step-change innovations when data are combined. For example, standardized soil methods allowed

108 for 100 m scale mapping across the United States, enabling detailed human–landscape models that can aid in preserving vital soil

109 resources (Ramcharan et al., 2018). In the field of rock mechanics prior to the 1950s, theoretical developments of rock failure and

110 plasticity lagged other branches of geophysics and engineering. It is likely that progress was limited not only by technology but,

111 arguably more so, by lack of consistent methods. Methods for repeatable failure testing were then developed, largely in the groups

112 led by Knoppf, Griggs, and Turner in the United States and Australia (Wenk, 1979). This standardization culminated in the

113 landmark series of papers that comprised the observations driving 50 subsequent years of experimental rock mechanics (e.g., Borg

114 and Handin, 1966; Handin et al., 1963; Handin and Hager, 1957, 1958; Heard, 1963; Mogi, 1967, 1971; Turner et al., 1954).

115

116 **1.2 Existing fracture measurement approaches across disciplines**

117 For the specific case of fracture-focused research, outside of geomorphology applications, the need for standardized rule-based

118 methods has already been established. Within this prior body of research, engineering and structural geology applications have

119 dominated the development of various approaches.

120

121 Engineering geology and geotechnical engineering share common practices in mapping different standards of rock quality and

122 rock mass classification, of which fracture characterization is an important component. The rock quality designation (RQD) was

123 developed in the early 1960s to predict rock mass suitability for building, foundations, tunneling, and other geotechnical issues

124 (Deere, 1964 in Bell, 2007). Within that work, the primary concern is the integrity of the rock, which is governed by its

125 discontinuities, primarily fractures. By providing a standard approach to defining rock quality - albeit qualitative or semi-

126 quantitative - the development of a globally accepted basis of rock mass classification built from RQD and discontinuity surveys

127 has provided a common language for engineering geologists and geotechnical engineers to discuss site suitability and to design

128 critical infrastructure to the point that slope stability parameters, hydrologic suitability and intact strength can be broadly predicted

129 (Bell, 2007; Hencher, 2012; Hencher, 2015). Thus, such rock quality metrics may be appropriate for surface processes applications,

130 and they provide a rationale and basis for the use of the semi-quantitative methods presented herein.

131

132 The rock quality index consists of qualitative classifications from very poor (RQD 0 to 25%) to excellent (RQD 90 to 100%) based

133 on the linear fracture frequency in core or outcrop line surveys, laboratory velocity measurements, or the ratio of the deformability

134 of the rock mass to that of intact rock (Bell, 2007). Specifically for fractures, rock quality designations are derived only from counts

135 of the number of fractures per foot or core or outcrop. More quantitative estimates of outcrop rock mass quality – commonly used

136 to estimate slope stability quantities – involve measuring multiple lines on an outcrop with estimates of fracture aperture width,

137 hydrologic state (closed, cemented, partially open, open and flowing), fracture orientation, strength of intact rock estimated with a

138 rock hammer, degree of weathering, and fracture 'roughness' or relief along a line of a fixed length, commonly 20 m to 30 m (Bell,

139 2007). These surveys are then repeated periodically with a spacing of ~100 m, depending on the application (Bell, 2007). Similar

140 methods are used with core and image logging tools (Hencher, 2012; Hencher 2015). The fracture parameters are then used in a

141 variety of index models that predict the bulk strength, hydraulic conductivity, and stability of the rock mass. Thus, the extensiveness

142 of the list of measured rock- and fracture- characteristics in the geotechnical engineering literature reflects the variety of impacts

143 that they have both on each other and on the behavior of the rock mass. Here a similar comprehensive list is proposed, but more

144 with surface processes applications in mind, and thus applicable to a larger range of scale of fractures.

145

146 Measurements of the length and aperture of fractures that intersect a line (scanlines), similar to those used for engineering rock

147 quality applications, are widely used and effective in structural geology applications (Marrett et al., 2018; Hooker et al., 2009),

148 and may be valuable where exposures approximate a 1D sample. Selection bias can be avoided by randomly picking scanline

149 directions or by measuring multiple scanlines. To capture all fracture orientations geometric corrections are needed (e.g., Terzaghi,

150 1965; Wang et al., 2023). When fractures are oblique to scanlines, these corrections are generally more effective if scanlines are

151 long relative to fracture occurrence. Calculations of fracture number density and fracture intensity (Section 6.1) require corrections

152 for comparison with 2D data. Depending on the heterogeneity and anisotropy of host rocks, long 1D measures may complicate

153 comparison of fracture patterns to rock properties. Although they are well suited for capturing the most reproducible and unbiased

154 measure for fracture size, namely fracture aperture distributions (e.g., Marrett et al., 2018) as a 1D measure, without extra

155 measurement steps, scanlines are not well suited for characterizing representative 2D or 3D rock characteristics or for measuring

156 fracture lengths, heights, or connectivity, all important to surface processes. Thus, in the proposed methods herein, the focus is on

157 2D 'windows', and an expansion of fracture length measurements – like that proposed by Weiss (2008) – is also detailed so that

158 long fractures are not underrepresented (Section 5.4.1).

159

160 For 2D characterizations, Zeeb et al. (2013) sought to determine how different sampling approaches lead to censoring bias of

161 different fracture sizes from outcrop data by applying different sampling methods to artificially generated fracture networks that

162 had known parameters. Analysis of data collected using scanline, window, and circular estimator methods revealed that the window

163 approach resulted in the lowest uncertainty for most parameters and required the fewest measurements to provide representative

164 datasets. For areas with large outcrop exposures, circular scanlines combined with a window approach have proven effective

165 (Watkins et al., 2015). Scanlines are also helpful in characterizing simple fracture spatial arrangement attributes. Here, a 'window'

166 approach is outlined that can be employed regardless of outcrop size or fracture number density, both of which could vary

167 considerably in any given surface process field area.

168

169 Another consideration that arises in both structural geology and the engineering applications is that the methods of fracture (and

170 rock) characterization must include accommodation for rock variations, and discipline-specific considerations for specific sites

171 (Hencher, 2012). In particular, the total area(s) of observation and numbers of fractures examined must always be normalized for

172 the specific rock and/or location within the 'fracture stratigraphy' of a study (e.g., Laubach et al., 2009). For example, it is common

173 for sandstone and shaly sandstone to both occur over short distances, and that their fracture abundance will vary by rock type (for

174 example, clay-poor sandstones tend to be more brittle and fracture prone). In this circumstance, the lithologic control on abundance

175 is identified first (this can be qualitative), then the abundance measures are normalized to area of the specific rock type. For

176 example, Hooker et al. (2013) employs a reverse procedure, whereby multivariate measures are used to isolate the rock type to

177 which normalization should be confined (if any). A further caution is that all fracture populations in the same rock may not reflect

178 the attributes of the host rock in the same way (all parts of the fracture population may not even be present in all rock types). This

179 variance may arise if fractures are not all the same age; because differences in loading paths, exposure histories, and rock properties

180 may vary. Engineering geology applications often map fracture populations in a similar way (Hencher, 2012; 2015) but without

181 the geologic context. Instead, zones are identified and cross-cutting relationships of fractures are commonly used to identify

182 primary vs. secondary planes of weakness. The methods presented herein include instructions for how to make these overall

183 judgements of necessary accommodations and normalizations.

184

185 Just as fracture characterization methods must be developed to accommodate variance between and across rock types, they must

186 also be developed so that they are reproducible across users. Above all, it has been established that reproducibility requires clear,

187 rule-based criteria for all decision-making (Forstner and Laubach, 2022). Forstner and Laubach (2022) and Ortega and Marrett

188 (2000) detail issues that arise, particularly from a lack of specificity with respect to identifying features to be measured. In another

189 case example (Andrews et al., 2019), study participants were asked to measure fractures with no particular instructions given for

190 how to collect the data other than where to collect it. The wide variance in resulting datasets collected by different users led to the

191 conclusion that, without common and clearly established measurement and selection criteria, fracture characterization is rife with

192 subjective bias that severely impacts interpretations of results. Then, based on post-data collection interviews and workshops,

193 Andrews et al. (2019) scrutinized the source of the variance and provided a list of suggested best-practices that would serve to best

194 eliminate the subjectivity of data collection that was leading to the bias. In engineering contexts, it is more common to handle such

195 possibility of bias by having fracture mapping during site investigations be performed by a single engineering geologist or by a

196 single, small team of trained engineers or geologists (Hencher, 2012). Ideally, either would be carefully reviewed by a senior

197 engineering geology professional. These fracture maps are incorporated into the site model, which is updated – preferably by the

198 same engineering geologist – during construction. In case studies, it is common for poor quality or inconsistent fracture mapping

199 to lead to incorrectly designed structures, which may fail (Hencher, 2012). Despite these often-dramatic failures, the site-specific

200 nature of fracture networks during rock mass characterization and the balance for a financially successful project may lead to poor

201 review and oversight practices while developing a site model (Hencher, 2012). Here, so that users from different groups may

202 consistently employ this field guide, clear, rules-based criteria are provided that may be used for all measurements described and

203 justify the criteria based on past work and experience.

204

205 Including that described above, incorporated in this work are suggested best practices from existing published methods research.

206 For example, field measurement 'crack comparators' are effective for measuring opening displacements particularly for sub-

207 millimeter widths (e.g., Ortega et al., 2006). Other measurements such as length and connectivity may have low reproducibility

208 (Andrews et al., 2019) owing to various observational and conceptual problems, including dependence on scale of observation

209 (e.g., Ortega and Marrett, 2000).

210

211 In addition to existing field based fracture research, remote sensing technologies such as lidar, drone photogrammetry, and structure

212 from motion, are becoming increasingly common to enable the production of fracture maps whose properties can then be quantified

213 and characterized digitally using freely available software packages such as FracPaQ (Healy et al., 2017). These technologies are

214 rapidly evolving and hold great promise for expanding the scope of fracture measurements overall (e.g. Betlem et al., 2022; Zeng

215 et al., 2023). To date, however, mapping fractures using these techniques holds limitations such as difficulty distinguishing between

216 fractures and edges, and are not readily accessible to all field scientists. We believe that it would be premature, and is also beyond

217 the scope of our goals, to try to distill those methods into best practices. Instead, we assert that the methods outlined herein represent

218 a consistent set of methods that could be employed for validation across all such remotely sensed data collection. Furthermore,

219 many of the field methods described herein, such as site and observation area selection, are required for any fracture mapping

220 effort regardless of technique. Thus, many of the methods we present can be applied to most studies using these rapidly evolving

221 remote sensing technologies and should aide in accelerating their development.

222

223 Finally, in all cases, the chosen standardized methods presented are optimized for collecting outcrop- and clast-fracture data

224 relevant to geomorphology and other surface process-based disciplines (e.g. critical zone sciences, building stone preservation,

225 hydrogeology). The methods described herein are germane to surface and near-surface (< 0.5 km) studies such as validating

226 geophysical measurements, testing factors that influence fracture formation, or documenting links between fracture characteristics

227 and topography or sediment production. Due to a lack of explicit knowledge suggesting otherwise, we present these methods based

228 on an assumption that fractures of all scales (um to km) contribute to all surface processes. Thus, these methods may differ from

229 those of studies with other goals, such as using outcrops as analogs for deep (km scale) subsurface fractures. Such studies aim to

230 distinguish mechanical and fracture stratigraphy, corroborate fracture patterns related to features (i.e., folds or faults), obtain

231 fracture statistics for discrete fracture models (Sect. 1.3), or test efficacy of forward geomechanical fracture models. For these

232 studies applied towards understanding deeper deformation, mineral filled fractures may be more useful or appropriate than focusing

233 solely on open fractures. Also, for deep-Earth applications, near-surface and geomorphology-related fractures are considered

234 "noise" and need to be omitted (e.g., Sanderson, 2016; Ukar et al., 2019). Yet, fractures that are noise to those interested in the

235 deep subsurface are essential features in the context of geomorphology and critical zone sciences. A major outstanding question is

236 how this differentiation might be reasonably and accurately accomplished given the relatively sparse number of studies of fractures

237 in the context of geomorphology. We hope future workers using this guide may find the answers.

238

239 **1.3 Existing fracture modeling and statistics methods**

240 Once fracture field data is collected, the metrics of its distribution can provide important insights into fracture processes (e.g.

241 Ortega et al., 2006). For example, power law distributions can be employed as a conservative rule of thumb for determining if

242 enough fractures have been measured (Sect. 4.2). Importantly, however, not all observations of fracture characteristics will be

243 power-law distributed, with other heavy-tailed distributions possibly indicating other, less random controls on fracture properties;

244 this is quite technical, and the reader is referred to Clauset et al (2009). If the data set is power-law distributed, however, then the

245 power law exponent – the slope of the distribution in log-log plots—is the key parameter that determines the distribution of different

246 fracture geometries. While it is tempting to just plot the data on a log-log plot and fit a line, this approach has proven to produce

247 incorrect, strongly biased estimates. Again, without performing correct, unbiased statistical analysis, it is not possible to compare

248 the power-law behavior and other statistics between different, carefully, and time-intensively collected data sets, limiting how

249 generalizable the results are. It is an interesting and largely unaddressed question the extent to which they may be applicable in

250 surface process-based fractures studies. Thus, for convenience, we outline the details of two straightforward, alternative approaches

251 that have been developed for other, deeper-Earth applications that surface processes workers may test on their own data.

252 To understand fracture length and fracture width data, it is key to first recognize that, with the exception of studies such as in rocks

253 with fractures with uniform spacing and bedding-controlled widths (Ortega et al., 2006), the data can commonly have a heavy-

254 tailed distribution, such as lognormal, gamma, or power law. As mentioned above, of these, strong observational and theoretical

255 evidence suggests that fracture size is commonly power law distributed (e.g., Bonnet et al., 2001; Davy et al., 2010; Hooker et al.,

256 2014; Ortega et al., 2006; Zeeb et al., 2013), i.e.,

257
$$n(b) = Ab^{-\alpha} \tag{1}$$

258 where b is the fracture dimension (length or width) of interest, n is the number of fractures with dimension d, and A and α are

259 constants. When log-transformed, Eq. (1) becomes

260
$$\log(n(b)) = \log(A) - \alpha \log(b) \tag{2}$$

261 which has led many practitioners to fit Eq. (2) by linearly binning the data in n, then log-transforming the data and fitting the

262 resulting data with a linear regression. This has proven to lead to significant bias in estimates, $\hat{\alpha}$, of the power law exponent

263 (Bonnet et al., 2001; Clauset et al., 2009; Hooker et al., 2014) and is not recommended despite its common usage.

264 Two straight-forward approaches have been shown not to have biases, or misestimates of the exponent α. 1) The following is based

265 on Clauset et al. (2009). First, the exponent can be found from the cumulative distribution of the dimensions, C(b), or number of

266 fractures with dimension greater than b, i.e.,

267
$$C(b) = \int_b^{b_{\max}} n(b) db \tag{3}$$

268 Where $b_{\max}$ is the maximum size of the fracture dimension (e.g., maximum length or width). The cumulative power law distribution

269 has the form

270
$$C(b) \propto b^{1-\alpha} \tag{4}$$

271 It is common to denote 1-α as c. To find α (or c), the dimension data is logarithmically binned. In other words, the dimension data

272 is binned on a logarithmic (1, 10, 100, …) frequency scale, and then log-transformed. At this point, linear regression techniques

273   can be applied to estimate α and assess uncertainty. However, in all cases, uncertainty estimates such as R^2 will overestimate the
274   certainty for such log-transformed data; but at least the estimate of α is unbiased.

275   2) Another method to find α from a data set of fracture dimensions is to use the maximum likelihood estimator (MLE) given by

276

$$\hat{\alpha} = 1 + N\left[\sum_{i=1}^{N} \ln\left(\frac{b_i}{b_{min}}\right)\right]^{-1} \tag{5}$$

277   where $\hat{\alpha}$ is the estimate of the exponent in (1), b_i is the dimension of the ith fracture, b_{min} is the minimum valid fracture dimension
278   (see below) and N is the total number of samples (Clauset et al., 2009; Hooker et al., 2014). The MLE estimate has the advantage
279   of an accurate estimate of standard error, σ, given by

280

$$\sigma = \frac{\hat{\alpha}-1}{N} + O\left(\frac{1}{N}\right). \tag{6}$$

281   Clauset et al. (2009) showed that both the logarithmically-binned cumulative distribution and the MLE estimator produce unbiased
282   estimates of the exponent. For all empirical power law distributions, there is a scale; in this case b_{min}, below which power law
283   behavior is not valid. This can be visually assessed by plotting Eq. 2 with logarithmically binned n. The interval between b_{min} and
284   b_{max} where the slope is linear is where the power law is valid (Clauset et al., 2009; Ortega et al., 2006), and Clauset et al. (2009)
285   presents a formal method to find b_{min} and b_{max}. Hooker et al. (2014) use a chi^2 test to evaluate the goodness of fit, which is simpler
286   than the p-tests of the Kolmogorov-Smirnov statistic proposed by Clauset et al. (2009).

287   **2 Guiding Principles**

288   **2.1 Natural rock fracturing background**

289   The design of any fracture-related study in the context of surface processes must arise from consideration of the variables that may
290   influence the rates of fracturing and the characteristics of the fractures that form. When rock is proximal to Earth's surface, those
291   variables include factors related to Earth's topography, atmosphere, biosphere, cryosphere, and/or hydrosphere. Here, a very brief
292   overview is provided of some key rock fracture mechanics concepts behind these factors. Eppes and Keanini (2017) and Eppes
293   (2022) provide more detailed reviews of rock fracture and fracturing processes in the context of surface processes.

294

295   Rocks fracture at and near Earth's surface in response to the complex sum of all tectonic (e.g., Martel, 2006), topographic (e.g.,
296   St. Clair et al., 2015; Moon et al., 2020; Molnar, 2004), biological (e.g., Brantley et al., 2017; Hasenmueller et al., 2017), and
297   environment-related (e.g., Matsuoka and Murton, 2008; Gischig et al., 2011) stresses they experience. Fracturing can occur when
298   stresses exceed the failure criteria (i.e., short-term material strength). More commonly, however, because critical stresses are rarely
299   reached in nature, fractures can also propagate *subcritically* at stresses as low or lower than 10% of the rock's strength (see
300   textbooks such as Schultz, 2019; Atkinson, 1987).

301

302   Overall, subcritical fracture propagation rates and processes are strongly dependent on stress magnitude, but they are *also* strongly
303   influenced by the size of the fracture that is under stress (see fracture mechanics textbooks such as Anderson, 2005; or reviews
304   such as Laubach et al., 2019). For single isolated fractures, stresses applied to the rock body are concentrated at fracture tips
305   proportional to the length of the fracture (a concept embodied by the term 'stress intensity'), effectively increasing the stresses

306 experienced by that fracture. Simultaneously, as the entire group of fractures within the rock body grows, the rock can become

307 'tougher' – more resistant to further brittle failure under the same magnitudes of stresses, as the total rock mass becomes more

308 compliant (Brantut et al., 2012). Overall, the time-dependency of these interacting and contrasting behaviors is not well

309 characterized in natural settings - deep, shallow or surface.

310

311 In addition to fracture geometry, environmental conditions also strongly impact fracture tip bond breaking during subcritical

312 fracture. The environmental factors known to impact subcritical rock cracking - separate from their influence on stresses - include

313 vapor pressure, temperature, and pore-water chemistry (Eppes and Keanini, 2017; Eppes et al., 2020; Brantut et al., 2013; Laubach

314 et al., 2019). Therefore, in the context of surface processes, climate matters twice for rock fracturing: 1) as it contributes to the

315 stresses that the rock experiences, and 2) as it contributes to the chemo-physical processes that break bonds at fracture tips as they

316 propagate subcritically.

317

318 Just as other common physical properties like tensile strength can be measured, rocks can be tested for their propensity to fracture

319 subcritically by the measurement of subcritical cracking parameters such as the subcritical cracking index (e.g., Paris and Erdogan,

320 1963; Chen et al., 2017; Holder et al., 2001; Nara et al., 2012; Nara et al., 2017). These parameters influence both the rate of

321 subcritical cracking in rock and the fracture characteristics (e.g., amount of fracture per area or fracture length as in Olson, 2004).

322

323 In sum, natural rock fracturing is not necessarily the singular, catastrophic event, as it frequently portrayed in surface processes

324 research. Instead, it is likely dominantly a slowly evolving process progressing over geologic time as has been recognized from

325 fracture patterns in bedrock (e.g. Engelder, 2004; Rysak et al., 2022), and more recently in the context of surface processes

326 (Shaanan et al., 2023). Importantly, however, there is currently little field-based data elucidating these complex, experimentally

327 observed phenomena in surface processes contexts. It is therefore our hope that this guide will enable more workers to document

328 the complex feedbacks between rock and fracture properties, as well as environmental, topographic, and tectonic factors, that likely

329 influence all fracturing at and near Earth's surface.

330 **2.2 Study design and site selection using a "State Factor" approach**

331 Due to their influence on rock fracturing as described above, all potential driving stresses and variations in fracture environments

332 must be considered in study design and site selection for any fracture-related research. Parent rock, topography (and other loads),

333 climate, biota, and time all potentially impact initiation and propagation of surficial fractures in rocks. Though this idea might

334 generally exist in other fracture-focused research, in the field of soil geomorphology it has long been explicitly described as a

335 'State Factor' approach (e.g., Jenny, 1941; Phillips, 1989) to understanding progressive chemical and physical alteration processes.

336 Thus, we propose that this well-vetted conceptual paradigm may be employed in fracture-focused surface processes research as a

337 standard.

338

339 Here, it is asserted that applying a State Factor approach to fracture research is relevant because fracturing processes are influenced

340 by each of these factors, just as all other chemical processes acting on rock and soil. This is particularly true when the subcritical

341 nature of rock fracture is considered (Sect. 2.1). Thus, all State Factors that could contribute to fracture propagation styles, and

342 rates should be explicitly considered and controlled for as much as possible within the aims and scope of the research for any given

343 site. These 'State Factors' - long categorized as they relate to overall soil development, of which physical weathering is a

344 component (e.g., Jenny, 1941) - are equally applicable to fractures alone, and include climate (cl, both regional climate and

345 microclimate), organisms (o, flora and fauna), relief (r, topography at all scales), parent material (p, rock properties) and time (t,

346 exposure age or exhumation rate). For rock fracture, tectonics (T) should be added to this list, making cl,o,r,p,t,T.

347

348 Hereafter, the term 'site' refers to a single location of either a group of rock clasts or a group of outcrops, whereby all clasts or

349 outcrops within the 'site' could be reasonably assumed to have experienced similar State Factors over their exposure history. For

350 example, a site might comprise a single boulder bar on an alluvial fan surface or a single ridgeline with several outcrops. Once the

351 specific State Factors (including the internal variability of each site) are identified for all the sites within a given field area, a series

352 of sites can be selected whose State Factors are known and controlled for as much as possible. This enables a study of the influence

353 of individual factors across the sites, i.e., fracture chronosequences, climosequences, toposequences, or lithosequences.

354

355 For rock fracture, it is important to understand how each cl,o,r,p,t,T factor may contribute both to stresses that give rise to fracturing,

356 and/or to the molecular-scale processes that serve to subcritically break bonds at fracture tips (Sect. 2.1). Based on existing

357 experimental data and weathering research, and without evidence to show otherwise, we infer that each has the potential to

358 independently impact fracturing rates, styles, and processes in surface processes contexts. The following descriptions provide only

359 brief examples from that literature as to how each of the State Factors may influence rock fracture. To fully describe each of their

360 influences on rock fracturing generally would comprise a textbook. Assuredly, to date, there are insufficient data to propose a

361 hierarchy of their influence on fracture characteristics in surface processes contexts. The factors are therefore listed in the

362 cl,or,r,p,t,T order by traditional convention only.

363 2.2.1 Climate (cl)

364 *Climate (cl)* as a State Factor refers not just to regional mean annual precipitation or temperature, but also the local microclimate

365 of a site, which may be influenced by site characteristics, such as runoff or aspect. The presence of liquid water increases the

366 efficacy of water-related stress-loading processes like those related to freezing (Girard et al., 2013) or chemical precipitation of

367 salts or oxides (e.g., Buss et al., 2008; Ponti et al., 2021). Moisture – particularly vapor pressure – can also serve to accelerate rock

368 fracturing rates independent of any stress-loading (e.g., Eppes et al., 2020; Nara et al., 2017). Temperature cycling can produce

369 thermal stresses (through differential expansion and contraction of both adjacent minerals as well as different portions of the rock

370 mass, e.g., Ravaji et al., 2019), and can also influence rates and processes of fracture-tip bond breaking (e.g., Dove, 1995).

371 2.2.2 Organisms (o)

372 *Organisms (o)* refers to both flora and fauna - everything from overlying vegetation and large animals to roots and microorganisms,

373 all of which may provide a source of rock stress and/or may influence water availability or chemistry. These relationships can be

374 complex and unexpected. For example, tree motion during wind and root swelling during water uptake both exert stresses on rock

375 directly (Marshall et al., 2021a). Organism density and type can impact rock water and air chemistry (Burghelea et al., 2015), both

376 of which may impact the rates and processes of subcritical cracking (e.g., review in Brantut et al., 2013).

2.2.3 Relief (r)

In the context of State Factors, *relief (r)* refers generically to all metrics related to topography including aspect, slope, and convexity. Topography impacts the manifestation of both gravitational stresses. as well as tectonic stresses within the rock body (Molnar, 2004; Moon et al., 2020; Martel, 2006). The directional aspect of a particular outcrop or boulder face may also influence insolation and water retention, translating into differences in microclimate and vegetation and, thus, weathering overall (e.g., Burnett et al., 2008; West et al., 2014; Mcauliffe et al., 2022), including fracturing (e.g., West et al., 2014).

2.2.4 Parent material (p)

The *parent material (p)* factor in the context of a fracture study refers to the specific rock type(s) containing fractures (and potentially undergoing fracture) in the geomorphic environment. Rock varies in the types and dimensions of material present (e.g., sandstone, siltstone, shale, basalt, granite etc.) and the types and spatial arrangements of interfaces within the material (e.g., grain size, porosity, bedding, foliation). These properties directly influence the rates and styles of fracture propagation (Atkinson, 1987) due to both how they respond to stresses but also due to how they allow stresses to arise (e.g. through their compliance, thermal conductivity, etc.). Thus, different rock properties differently influence the rates and characteristics of fracture growth and susceptibility to topographic and environmental stresses. For example, different minerals are characterized by different coefficients of thermal expansion. As a result, rocks with different mineral constituents will be more or less sensitive to thermal stresses than others depending on the contrasts between adjacent grains. Rock mineralogy will also impact chemical processes acting at crack tips during subcritical cracking, as well as the overall susceptibility of the rock to chemical weathering.

Many (perhaps most) rocks contain fractures that formed prior to exposure, either due to deep seated tectonics and fluid pressure loads or to thermal and mechanical effect due to uplift towards the surface (English and Laubach, 2017; Engelder, 1993). In sedimentary rocks, fracture patterns (and, in some cases, fracture stratigraphy) vary with mechanical stratigraphy (e.g., Laubach et al., 2009) that can also influence near-surface fracture. In many instances, mechanical properties may be reflected in fracture stratigraphy, and vice versa. Schmidt hammer measurements are a useful, fast, and inexpensive field approach to documenting mechanical property variability (Aydin and Basu, 2005), however such measurements are impacted by weathering exposure age (e.g. Matthews and Winkler, 2022). The influence of fracture characteristics of the parent rock that may have formed in the deep subsurface are described in Sect. 2.2.6 "Tectonics".

Additionally, in the context of surface processes studies, we propose that parent material also refer to the size and shape of the clast or outcrop. Because, for example, angular corners generally concentrate stresses more than rounded edges (Anderson, 2005). Also, clasts or outcrops of different sizes experience different magnitudes of thermal stresses related to diurnal heating and cooling (Molaro et al., 2017).

2.2.5 Time (t)

Time (t) likely plays a role in rock fracturing rates just as it does in chemical weathering, whereby outcrops found in slowly-eroding environments or clasts on old surfaces may be subject to different fracturing rates and processes (e.g., Rasmussen et al., in review; Mushkin et al., 2014). Over time, rock mechanical properties can also change as weathering occurs (e.g., Cuccuru et al., 2012). Although the time factor has not been well-studied in the context of natural rock fracture, preliminary data suggest that it should

413   be considered (Berberich, 2020; Rasmussen et al., 2021). Published surficial geologic maps or datasets of rock exposure ages or
414   erosion rates (e.g., Balco, 2020) can provide 'time' information.

415   **2.2.6 Tectonics (T)**

416   Finally, in a fracture-related study, *tectonic (T)* setting must also be considered as a State Factor. Fractures that have formed in the
417   deep to near subsurface in response to tectonic forces such as plate-scale stress fields, folding, and faulting (and attendant pore
418   pressure variations) may continue to propagate at or near the surface, and they inevitably become exhumed. Overall, fractures
419   formed by these processes have traditionally been studied within the structural geology discipline, and that literature is extensive
420   (e.g., reviews in Laubach et al., 2019; Laubach et al., 2018; Atkinson, 1987, Chapter 2). The tectonic history of rock can be recorded
421   or manifest in its brittle structures that are then maintained over a wide range of past tectonic events, including its most recent
422   exhumation and cooling. The attributes of resulting open or filled fractures depend on how deeply the material was buried, how
423   rapidly uplifted, and the material properties (e.g., English and Laubach, 2017). Finally, the fact that the current tectonic setting can
424   drive ongoing deformation has long been recognized (e.g., Hooke, 1972), and more recent work has highlighted that very low
425   magnitude tectonic stresses can translate to fracture propagation in very near-surface bedrock, especially when interacting with
426   local topography (e.g., Martel, 2011; Moon et al., 2020).

427

428   It is likely, though perhaps not widely appreciated, however, that fractures originally opened due to tectonic stresses further
429   propagate, not only due to ongoing tectonic stresses as they approach the surface, but also due to topographic and environmental
430   stresses that the rocks increasingly encounter as they are exhumed to shallower depths. Simultaneously, these 'new' stresses may
431   increase the overall number density (total number of fractures per area) and fracture intensity (defined here as total fracture length
432   per area). These changes in fracture characteristics may manifest abruptly with depth or more gradually and those changes may
433   manifest differently under different topographic portions of the landscape (e.g., ridges versus valleys). There is a growing body of
434   data pointing to such surface interactions (e.g., Marshall et al., 2021b; Moon et al., 2019; Moon et al., 2020; St. Clair et al., 2015),
435   but overall, these differentiations are a topic ripe for further study.

436

437   Pre-existing fractures may not always be easily separable from those formed or further propagated under geomorphological
438   influence. Environmental stresses also produce parallel fractures (e.g., Aldred et al., 2015; Eppes et al., 2010; Mcfadden et al.,
439   2005), as do those related to the morphology of the eroding landscape (Leith et al., 2014). Thus, for outcrops, and particularly for
440   clasts where correlations or comparison with regional tectonic structures are not possible, fracture orientations may not uniquely
441   represent a tectonic regime. The non-geomorphic origin (or otherwise) of such fractures may be evident from microstructure
442   analyses that examines fractures for diagenetic cements, inconspicuous mineral deposits, fluid inclusions, or other similar features
443   (e.g., Ukar et al., 2019). Thus, in choosing study sites, consideration should be made of rock age, tectonic history and current
444   tectonic setting (e.g., World Stress Map, Heidbach et al., 2018), as well as unambiguously tectonically-related structures such as
445   dipping bedding planes, evidence of mineral deposits in the fractures, styolites, or ductile structures such as folds (Hancock, 1985;
446   Laubach et al., 2019).

447   **2.3 Bedrock outcrops versus deposited clasts**

448 The fracture characteristics of outcrops have long been employed as proxies for subsurface fracture networks, and there is a
449 reasonably large body of literature addressing these relationships and their potential pitfalls (e.g., Ukar et al., 2019; Al-Fahmi et
450 al., 2020; Sharifigaliuk et al., 2021). However, based on the growing body of research mentioned above, topographic and
451 environmental stresses both have likely contributed to any sub-aerially observed fracture network unless otherwise ruled out. Thus,
452 for studies that aim to isolate fractures associated with environmental stresses, measurements from clasts may be more useful than
453 outcrops.

454

455 Clasts that have been transported by fluvial, glacial, or mass-wasting processes have experienced abrasion, and therefore, it is
456 highly likely that pre-existing superficial fractures have been removed. Thus, clasts may be more reasonably considered 'fresh'
457 than an outcrop with an unknown exhumation history, allowing clearer linkages between environmental exposure and observed
458 fractures. This idea of "resetting" fractures within clasts through transport is supported by data showing clasts of identical rock
459 type that have experienced more transport (i.e., rounded river rocks) having higher strength than those found in, for example, recent
460 talus slopes (Olsen et al., 2020). Nevertheless, clasts may carry with them an invisible (to the unaided eye) population of pre-
461 existing fractures— or sealed microfractures—that do in some instances impart a strength anisotropy that can manifest in later
462 surface-related fractures, even in clasts. Thus, for such rocks, the 'reset' may be imperfect (e.g. Anders et al. (2014). In-depth
463 petrographic analysis to identify residual microstructures (e.g. ala Forstner and Laubach, 2022) may not be feasible in most
464 instances, but a simple uniaxial point load test, or field Schmidt-hammering of clasts found in active channels, may reveal if an
465 inherited anisotropy is present.

466 3 Selecting the clasts, outcrops, or rock surface locations that will comprise the fracture observation area

467 Carefully selecting the rock surface area(s) on which fractures will be observed and measured within a site is equally as important
468 as selecting the site or the fractures themselves. Hereafter, the term 'observation area' refers to the specific portion(s) of rock
469 surface(s) for which fractures are being measured. Observation areas may comprise the entire exposed surface of individual clasts,
470 outcrops, or portions of either (Fig. 1). In the following sections, instructions for selecting these observation areas in the field are
471 provided.

472 3.1 Establishing outcrop or clast selection criteria

473 Before observation areas can be identified, outcrops or clasts must be selected. The first step of that selection process is to establish
474 criteria for determining which outcrops or surface clasts within the site are acceptable for measurement. Without evidence to
475 proceed otherwise, similar to site selection, variability in cl,o,r,p,t,T factors that may influence fracturing (temperature, moisture
476 availability, rock shape, and rock type) should be controlled for as much as possible.

477

478 In general, characteristics of the clasts or outcrops that might impact mechanical properties, moisture, or thermal stress-loading
479 should be most heavily considered. The rock type properties that should be considered when developing selection criteria include
480 not only heterogeneities like bedding or foliation, but also grain size and mineralogy, all of which can influence fracture rates and
481 style characteristics. For example, perhaps only outcrops with no visible veins or dikes will be employed; or only outcrops greater
482 than 1 m in height; or only north facing outcrop faces. Past work, for example, has focused on upward facing surfaces of outcrops
483 or large clasts (e.g., Berberich, 2020; Eppes et al., 2018).

484

485 For loose clasts, only clasts of a particular size or rock type might be employed for measurement. For example, past work found

486 that below approximately 5 cm diameter in semi-arid and arid environments (Eppes et al., 2010), and 15 cm in more temperate

487 environments with vegetation (Aldred et al., 2015), clasts are more likely to have been moved or disturbed. Thus, these sizes were

488 employed as a threshold for selection.

489 **3.2 Non-biased selection of clasts or outcrops for measurement**

490 Once criteria are defined, clasts or outcrops meeting those criteria must be randomly chosen for the fracture measurements. A

491 procedure similar to the well-vetted Wolman Pebble Count style transect (Wolman, 1954) should be employed to avoid sampling

492 bias. For landforms with other geometries, a grid may be used instead of a transect line.

493

494 In either case, a tape transect or net grid is laid out on the ground at each site, and the clast or outcrop closest to specified intervals

495 on the tape (or at the points of the grid meeting the criteria) is selected (Fig. 1a). The interval or grid spacing should be adjusted to

496 the overall size and abundance of clasts or outcrops found on the surface. If there are relatively few meeting the criteria at a site,

497 all within the site meeting the criteria can be measured.

498

499 A similar technique can and should be applied for selecting outcrops. For example, care should be taken to not be limited to the

500 'best' outcrops (cleanest and/or largest), since they likely are the least fractured. However, such large, clean outcrops may be the

501 best places to observe any pre-existing subsurface-related fractures. For locations where outcrops are within a few meters or tens

502 of meters of each other and vegetation relatively sparse, a grid of a set dimension (e.g., 100 m) is overlain on aerial imagery, and

503 the closest outcrop to each grid intersection meeting the outcrop criteria are selected (Watkins et al., 2015). For areas where

504 outcrops are not visible in aerial imagery, a measured or paced transect can be employed where the user walks along a bearing and

505 chooses the closest outcrop meeting the selection criteria at each interval, e.g., 30 paces.

506

507 In all of the above, transect locations and orientations should be selected following consistent criteria and being mindful of the

508 State Factors cl,o,r,p,t,T. For example, all transects or grids might be placed uniformly along backslopes with a certain upslope

509 distance from the crest; or along the latitudinal center or crest of a landform. Alternatively, the transect might be orientated

510 perpendicular or oblique to a paleo-flow direction so that it is not constrained only to bars or swales. The coordinates and bearing

511 of all transects or grids should be recorded, enabling tracking and avoiding repetition.

512 **3.3 Observation areas comprising the entire clast or outcrop surface**

513 Fractures are three-dimensional objects, and ideally observations should encompass volumes; but, this is precluded by the opacity

514 of rock, so one- or two-dimensional observation areas must be used. Fracture arrays may also encompass a wide range of sizes, so

515 the selection of observation area(s) needs to consider truncation and censoring biases.

516

517 The observation area for small clasts and outcrops can be their entire exposed surface. In our experience, when clasts or outcrops

518 selected for measurements are less than ~50 cm in maximum dimension, measurements can typically be readily made for all

519 fractures visible on the clast or outcrop exposed surface for most rock types.

520

521 We strongly suggest that rocks should not be moved during measurement. This non-disturbance practice is particularly crucial for

522 maintaining Earth's geodiversity (Brilha et al., 2018) and preserving sites for future workers to revisit. Further, research examining

523 acoustic emission localization of rocks naturally fracturing found that the large majority of fracture 'foci' were located in the upper

524 hemispheres of boulders (Eppes et al., 2016). Thus, we infer that the potential insight gained by moving clasts does not warrant

525 the impact to geoheritage.

526 **3.4 Establishing 'windows' as the observation area for larger clasts and outcrops**

527 Particularly for larger exposures, it is not feasible to measure every fracture on an outcrop or clast. In these cases, the observation

528 area may comprise predetermined 'windows' of representative decimeter- to meter-scale areas of the rock surface (Fig. 1b). This

529 window selection method results in an accurate representation of fractures on an entire outcrop (e.g., Zeeb et al., 2013) and is least

530 affected by some subjective biases (Andrews et al., 2019).

531

532 Importantly, the number and size of windows observed on each outcrop or at each site should depend on the typical number and

533 size of fractures present on the surface of the rock (Sect. 4.2). Inevitably it is our experience that logistical constraints will dictate

534 that decisions must be made about size cutoffs. Some part of the smallest size fraction of fractures may not be readily visible, and

535 the finite size of exposures may mean that some large fractures are missed. Overall, it is preferable to strike a balance between

536 window size and number so that during data analysis, variance can be quantified by comparing data collected between windows

537 on the same outcrops and at the same site. More total observation area (e.g. more and/or larger windows) is required when fractures

538 are fewer per area. The size of the area required for a representative quantification of fractures depends both on fracture average

539 length and number density (e.g., Zhang, 2016). Here, an iterative approach is outlined for determining if sufficient area has been

540 examined (Sect. 4.2), but other rules of thumb exist, particularly in the Rock Quality Designation Index literature (e.g., Zhang,

541 2016).

542

543 Choosing the placement of windows on the outcrop should entail a stratified random sampling approach. Just as for clast- or

544 outcrop-selection, cl,o,r,p,t,T factors like aspect should be taken into consideration and controlled for as much as possible in the

545 window placement strategy by, for example, only using upward facing surfaces. Then, window placement determination is made

546 to avoid sampling bias and edge effects. For example, if upward facing outcrop surfaces are to be characterized, then the total

547 length and width of the face could be employed to align sufficient numbers of windows along even intervals of those measurements

548 (e.g., three windows whose centers are located along the center axis of the rock with even spacing between the edges and each

549 box; Fig. 1b).

550

551 For the placement of each window, it is our experience that a simple cardboard template of the appropriate window size with a

552 center hole can be employed to trace with chalk the window directly on the clast or outcrop. Then, all fracture measurements are

553 made in the window(s). Each window should be numbered and photographed in the context of each outcrop or clast. Also

554 recommended is detailed photo-documentation of each outcrop and transect, along with sufficiently detailed coordinates to

555 reoccupy the precise site (e.g. in meters or 0.00000 dd that are *always* referenced to the projection or datum used).

556 **3.5 How many observation areas?**

557 The number of clasts, outcrops, or windows required to measure sufficient fractures will vary with the study goals, site complexity,

558 and the variables for which the data are being tested or controlled. Importantly, for each study, the required number of observation

559 areas must be established based on the amount that is necessary to gain a statistically sufficient number of fracture observations to

560 represent the rocks in question for that setting (Sect. 4.2). Concepts of 'stationarity' have been applied in the context of 2D analyses

561 (e.g. Shakiba et al., 2023), but no rule-of-thumb in the context of surface processes is described herein because, as yet, there has

562 not been sufficient standard fracture data collected to establish such a rule. Establishing such a rule of thumb is an illustration of

563 the motivation of this paper, as well as an example of how the methods presented herein can and should evolve over time.

564

565 Rocks or outcrops with lower fracture number density (fewer overall fractures per area) will require that larger areas of their surface

566 be examined to measure sufficient fractures for statistical significance (Sects. 3.4 and 4.2). Rocks or outcrops with significant

567 variation in fracture patterns require sufficient observation to capture that variability. Thus, as an example only, in past work, when

568 State Factors were carefully controlled for, relationships between rock material properties and rock fracture properties were evident

569 from about three to ten meter-scale outcrops per rock type on ridge-forming quartz rich rocks (Eppes et al., 2018). However, until

570 sufficient magnitude of datasets have been collected for a particular site, the amount of observation area must be established based

571 on the number of fractures available uniquely at each study site.

572 **4 Selecting fractures for measurement**

573 **4.1 Rules-based criteria for selecting fractures in surface processes research**

574 The term 'fracture' is employed with a wide variety of meaning across the geosciences, potentially resulting in large variations in

575 the range of features that two individuals might study on a single outcrop (Long et al., 2019). Therefore, it is crucial to employ

576 clear and repeatable rules-based criteria (e.g., Table 1) for what constitute measurable 'fractures' within any fracture-related

577 research. Failing to do so consistently results in a high variance of subjective bias that is more reflective of worker personality than

578 of the variance in fracture of the outcrop (Andrews et al., 2019). Thus, consistency and documentation are required for deriving

579 interpretable and repeatable results.

580

581 The proposed rules (Table 1) for determining which fractures to measure at any given field site were developed by us in the context

582 of surface processes research and through iterations with numerous non-expert users (undergraduate students) to arrive at criteria

583 that provided consistency in observations across users. Because surface processes are frequently and largely dependent both on

584 rock erodibility and water within a rock body, the recommended criteria are applicable only to open voids, which are known to

585 greatly impact both. Also, because other types of open voids like vesicles are common in rock, additional criteria includes that the

586 open void must be planar in shape, bounded by parallel or sub-parallel sides (hereafter fracture 'walls'), with a visible opening that

587 is deeper than it is wide. Fracture walls commonly pinch together at fracture terminations.

588

589 Voids that fit the shape criteria that are filled with lichens, dust, or other permeable material that can be readily brushed out with a

590 fingernail or prodded with a needle should be included in the dataset. However, it is common for high length-to-aperture ratio

591 voids in rock to have been filled with cemented mineral solids during intrusion and metamorphism, diagenesis, or weathering.

592 Fractures, or portions of fractures containing these hardened cements, may become the hydrologic and mechanical equivalent of

593 solid rock. Although such filled and partly filled fractures may be key to describing fractures formed in the deeper subsurface, we

594 assert that fully cemented fractures do not meet the defined 'open' criteria relevant to surface processes studies, and in principle

595 should not be included in the fracture dataset. Where partly cement-filled fractures are present, specific rules may need to be

596 adapted to account for the pattern of cement such as counting segments of fractures that are separated by continuous mineral

597 deposits as separate features. If such a solid secondary mineral cement forms a discontinuous 'bridge' fully connecting the two

598 walls of an otherwise open, planar void, the open length of the fractures on either side of the bridge would be treated as individual

599 fractures. This partial 'bridge' or complete interruption of continuous fracture pore space is common in fractures that have existed

600 at elevated temperatures such as at depth or near hydrothermal features (see review in Laubach et al., 2019), so a yes/no indication

601 of their presence may be added to the dataset. A useful starting point for building such rules is to compare outcrops with

602 expectations for how mineral deposits are typically configured in partly cemented fractures (e.g., Lander and Laubach, 2015).

603

604 Finally, additional proposed criteria - based on our experience as well as fracture mechanics theory - is that the planar void must

605 be continuously open (no 'bridges' of cemented mineral material or of rock) for a distance longer than 10 times the characteristic

606 grain size dimension or 2 cm, whichever is greater. In most rock types, this translates to a 2 cm minimum cutoff for countable

607 fractures (Fig. 2a; see Sect. 5.4.1 for measuring lengths). This proposed length threshold is based on three features. First, past work

608 has demonstrated that deriving precise (repeatable) detailed information - other than length - for fractures <2 cm in length is

609 challenging (e.g., Eppes et al., 2010). Second, temperature-dependent acoustic emission measurements (Wang et al., 1989; Griffiths

610 et al., 2017) and theoretical arguments suggest that on single year time scales, fractures on single grain and smaller length scales

611 exist in thermodynamic equilibrium, randomly opening and closing under constant redistribution of ubiquitous diurnal to seasonal

612 thermal stresses within surface rocks. The approximate statistical mechanical 'rule-of-ten' states that well-defined equilibrium and

613 nonequilibrium, continuum-scale properties, e.g., viscosity, density, stress and strain, each determined by myriad microscale

614 random processes, are obtained on length scales approximately 10 times an appropriate molecular length scale, e.g., average atomic

615 size or mean free path length between colliding (gas) molecules. This interpretation is consistent with recommendations for the

616 number of grains the minimum diameter of a sample is for repeatable testing of continuous rock properties such as rock strength

617 and elastic moduli (e.g., ASTM, 2017).

618

619 Last, and practically, the high abundance of fractures below this cutoff significantly increases the time required for fracture

620 measurement. If these smaller fractures are of interest, they can be characterized with photographic analysis (not covered herein)

621 or subjected to semi-quantification via an index (Sect. 5.2).

622

623 Importantly, in some applications, it may be appropriate that a larger minimum threshold in fracture length is chosen. However, in

624 that case, fracture abundances in the rock will possibly dictate that significantly larger observation areas of the rock exposure need

625 to be employed in order to obtain sufficient numbers of fractures to provide representative data (Sect. 4.2).

626

627 Regardless of the threshold length chosen for the study, two adjacent fractures separated by intact rock or bridges of cement are

628 considered two fractures, even if at a distance they appear to be continuous (Fig. 2b). This practice results in repeatable

629 measurement between multiple workers and provides the most accurate representation of past fracture growth and fracture

630 connectivity in the rock body.

631 **4.2 Determining how many fractures to measure**

632 Most published fracture-focused studies provide no justification for the number of fractures they measure, begging the question -

633 is the dataset representative of the rock body? Studies of fracture statistics suggest a minimum of ~200 fractures (Baecher, 1983)

634 per site (as defined herein). For workers and situations that require more nuance or for which there is not ample rock surface to

635 examine, we recommend an iterative approach. It is a long-recognized concept in fracture and rock mechanics that fracture size

636 distributions are highly skewed and can be characterized by scale-independent power law distributions (e.g., Davy et al., 2010;

637 Hooker et al., 2014). Power law distributions cross multiple orders of magnitude in frequency and scale, requiring up to an order

638 of magnitude more observations to significantly define than the other, more tightly defined distributions. Thus, the best practices

639 to understand the commonly observed power-law distribution of fracture size can be leveraged in most cases to ensure that a

640 representative fracture population has been measured in any given dataset (Ortega et al., 2006).

641

642 Here, it is recommended that to fully characterize the fractures for any site(s), outcrop(s), or feature(s) of interest, sufficient

643 numbers of fractures should be measured such that, if the fracture parameters are power-law distributed, a statistically robust

644 power-law distribution (p-values <0.01) in fracture length or aperture can be estimated from the data. While other log-normal,

645 exponential, and Weibull distributions have been proposed for various fracture datasets (e.g., Baecher, 1983), employing these

646 distributions depends on preexisting knowledge of the expected dataset, the very data set in the process of being collected. Thus,

647 unless there is prior documentation of fracture distributions at a particular site, the power law distribution should suffice, and, in

648 any case, power law distributions require the most samples for significance compared to the other distributions.

649

650 Thus, in practice, it will be an iterative process to determine the number of fractures required for any given dataset; but generally,

651 on the order of 10^2 fractures are required (e.g., Zeeb et al., 2013) to reach a representative distribution (Fig. 3). When sufficient

652 numbers of fractures have been measured to result in such a distribution, then it can be assumed that the population of measured

653 fractures is representative of all fractures on the rock, outcrop, or group of rocks/outcrops with certain features. For example, if the

654 goal of a study is to test the influence of rock type on fracture density, enough fractures must be measured to allow for a power-

655 law distribution of fracture size for *each* of the rock types. That population of fractures can then be considered representative of

656 the given rock type, and statistics on other fracture properties like width can also be reasonably interpreted as representative.

657

658 If after ~200 fractures are measured the power law distribution is not met, then it is likely the dataset does not follow a power-law

659 distribution and the number of measurements can be considered sufficient (Baecher, 1983). Some fracture arrays – particularly

660 those formed at depth - have narrow (or 'characteristic') size distributions that are not well approximated by power laws (e.g.

661 Hooker et al., 2013). Another exception to the scale independent power law rule of thumb may be if there are abundant fracture

662 terminations in infilling material. In this case, the size of the fracture (as defined by Table 1) is dictated by the spacing of the filled

663 material bridges. Thus, fracture sets in rocks that contain abundant varnish or secondary precipitates like calcium carbonate may

664 not follow the power-law rule, and a threshold number of ~200 fractures per site should be employed.

665

666 An example of what the iterative process might look like is found in Fig. 3. In this example, all fractures were measured on the

667 surface of 15-50 cm diameter granitic clasts selected along transects across both a modern wash bar (with few overall fractures per

668 clast) and a ~6 ka alluvial fan bar (with many fractures per clast). For the modern wash, after 5, 30, or 50 clasts, a statistically

669 significant power law distribution is not evident (Fig. 3). However, after 130 clasts, the fit of the power law falls below a p-value

670 threshold of 0.01 with 111 fractures measured. Thus, measurements from around 130 clasts (~100 fractures) were necessary to

671 fully characterize fractures for that particular site. In contrast, the threshold p-value is reached after only 5 clasts (64 fractures) for

672 clasts with high fracture number density on the mid-Holocene age site; however, with more clasts examined, more variables per

673 clast can be analyzed in the data. Thus, in order to evaluate different variables (like clast size or shape), the iterative process would

674 repeat, but limiting the analysis to fractures found on clasts meeting the criteria of interest. In this example, a total of 130 clasts

675 per surface were measured, enabling several subsets of data to be examined in order to test the influence on a range of clast

676 properties on fracture characteristics. This iterative approach will give a reasonable assurance of when enough samples have been

677 collected, but determining the type of distribution and estimating the distribution parameters, i.e., the exponent of the power-law,

678 require more careful analysis that is covered below in section 6.

679 **5 Proposed baseline field data for fracture-focused surface processes research**

680 Here, a basic suite of field data (Table 2) is proposed for all observation areas and all fractures. Table 3 contains a list of

681 recommended field equipment to make the measurements. The list of data in Table 2 was developed with the goal of allowing the

682 worker to fully analyze their fracture data in the context of variables known from the literature to influence or reflect fracture in

683 exposed rocks. Workers may choose to measure only some of these data if, for example, they have controlled for a particular metric

684 through site or clast selection. As overall knowledge of fractures in surface environments grows, the suggested set of measured

685 variables should also change, just as, for example, the components of the simple stream power equation have evolved in fluvial

686 geomorphology literature. The proposed fracture field methods list is also focused on direct 'observables' – without interpretation

687 – that should apply universally across field areas. We readily acknowledge that additional items can and should be added to

688 accommodate the needs of any specific study.

689

690 The metrics listed in Table 2, and the associated methods described below, are designed to be applicable and translatable to both

691 natural outcrops and individual clasts. While they may also be applicable to fractures found in quarries and road-cuts, such outcrops

692 are prone to fracturing that has been anthropogenically induced by blasting, exhumation, and new environmental exposure (e.g.,

693 Ramulu et al., 2009; He et al., 2012).

694 **5.1 The 'Fracture Sheet'**

695 A data collection template is provided that comprises all the proposed standard data, allowing efficient, complete, and detailed

696 recording of all parameters while in the field (e.g., a "fracture sheet", Fig. 4 with digital version provided in supplemental data).

697 The fracture sheet can and should be modified to include additional parameters relative to any study. The template provided here

698 is structured, based on our past experience, so that each observation area's information (e.g., that of each clast, outcrop, or window)

699 shares a row with the first fracture measured. Then, subsequent rows are employed for additional measured fractures on the same

700 observation area. Each observation area and fracture are assigned unique identifiers to enable unambiguous reference in subsequent

701 data analysis. Employing a 'window' rather than an entire clast or outcrop as the observation area necessitates slightly different

702 data collection, so two separate fracture sheets can be found in the supplement.

703

704 The fracture sheet provides a header space for site meta-data. Any observations that could elucidate the possible contributions of

705 any State Factor (cl,o,r,p,t,T) acting at the site should be recorded (e.g., the vegetation or topography of the site). This header area

should also be employed to note any and all criteria or conventions used throughout the study. For example, the use of any convention, such as right-hand rule for strike and dip measurements, should be noted in the header. The criteria employed to select clasts or outcrops (e.g., their size, composition, etc.) and the nature of the observation areas (e.g., only the north face of all clasts; or entire exposed clast surface for all outcrops) should also be noted.

5.2 The use of semi-quantitative indices

It is recommended that indices be employed for many observations following similar existing semi-quantitative methods commonly employed in both soil sciences (e.g., Soil Survey Staff, 1999) and sedimentology (e.g., rounding and sorting). We have found in our experience that the use of indices, rather than precise measurements, is especially appropriate for fractures and fracture characteristics given the natural variation between different rocks. Also, high numbers of small or discontinuous features on rock surfaces frequently precludes their accurate counting within a reasonable amount of time; for example, counting all fractures <2 cm in length.

Two particularly useful generic 'abundance' indices are defined here that are derived from those employed for quantifying the abundance of roots and pores in soils (Schoeneberger et al., 2012), whereby the quantity or coverage of specific elements or features is estimated within a specified area. For both, a 'frame' is employed whose size is dependent on the size of the feature being observed (Fig. 5). Features that are ≤0.5 cm are observed in 1 cm^2 frames; features >0.5 to <2 cm are observed in a 10 cm^2 frame; and features ≥2 cm are observed in a m^2 frame. Cut-out stencils of these sizes may be constructed and employed. The observer imagines randomly placing the 'frame' several times on any given portion of the observation area, noting the abundance of the feature of interest within the frame. The indices are based on the average value of abundance observed in any given such 'frame' across the entire area of observation (e.g., the entire clast, the entire outcrop, or the outcrop window).

The first index scales from 0 to 4 and is applicable for 'countable' features of interest in the research like small fractures, fossils, or large phenocrysts. The index is: none – 0 (no visible features in any frame), few -- 1 (<1 feature on average), common -- 2 (≥1 and <5 features on average), very common -- 3 (≥5 and <10 features on average), and many -- 4 (≥10 features on average).

The second index scales from 0 to 5 and is employed for features that are not readily counted nor consistent in size (like lichen, varnish, fine grained mafic, or felsic minerals). In these cases, the index is based on the percentage of the rock surface covered by the feature: none – 0; very little – 1 (<10%); little – 2 (≥10 and <30%); common – 3 (≥30 and <60%); very common – (≥60 and <90%); and dominant – 5 (≥90%). A percentage estimator (Fig. 6) should always be employed to assign the index categories – even experienced field workers are subject to 'quantity bias'.

5.3 Measuring rock characteristics

The following rock characteristics are measured for each observation area – each clast, outcrop, and/or window – that is employed in a study. Some fracture characteristics not captured in individual fracture measurements are also included. In particular, fracture connectivity and fracture spacing should be measured after all individual fractures within the observation area have been identified and measured.

741 **5.3.1 Clast, outcrop, or window dimensions**

742 Rock – or outcrop – size, aspect, and slope can impact stress-loading through, for example, thermal stress distribution (e.g., Molaro
743 et al., 2017; Shi, 2011). Or, for instance, natural outcrop height has been linked to its exposure age and/or erosion rates (e.g.,
744 Hancock and Kirwan, 2007; Anderson, 2002). The dimensions of the clast, outcrop, or window employed for fracture observations
745 are also required for calculations of fracture number density and intensity (i.e., the number/length of fractures per unit area; see
746 Sect. 6.1).

747

748 The length and width of planar 'windows' are measured directly. If a window 'bends' across multiple faces of the rock surface,
749 then separate length and width measurements should be made for each face with a distinct aspect. These areas are then added
750 together for fracture number density and intensity calculations.

751

752 The vast majority of rock clasts and outcrops found in nature have 'cuboid' forms (Domokos et al., 2020). Thus, length, width,
753 and height of individual clasts or outcrops may be reasonably employed to calculate the exposed surface area (see Sect. 6.1 for
754 calculations). If clasts or outcrops are well-rounded, spherical or half-spherical surface areas can be employed, depending on burial.

755

756 For all dimension measurements regardless of rock shape, metrics are measured as point-to-point orthogonal measurements. By
757 convention, length is measured parallel to the longest axis. Width is measured on the widest extent that is perpendicular to length,
758 and height is measured vertically from the uppermost surface of the rock down to the ground surface. In past surface processes
759 work (e.g. Aldred et al., 2016; Eppes et al., 2010; McFadden et al., 2005), we have developed the rule of thumb that if a through-
760 going fracture splits the rock into two pieces that remain *in situ*, it should still be considered one rock and measured accordingly.
761 Such fractures formed in place, and provide information about the fracturing history of the rock (e.g. D'arcy et al., 2014). If a clast
762 or outcrop is spheroidal in shape, that should be noted for future surface area calculations.

763

764 For site preservation, and to minimize geoheritage and environmental impacts, we believe that rocks should not be moved from
765 their natural state; therefore, the height measurement of a highly embedded rock will only represent the height of the exposed rock
766 surface above the ground. A metric derived to estimate the degree to which clasts are exposed versus embedded is provided in
767 Sect. 5.3.8.

768 **5.3.2 Sphericity and roundness**

769 Sphericity and roundness from standard sedimentology practices (e.g., Krumbein and Sloss, 1951) provide metrics for rock shape.
770 Shape can influence stress distribution in a mass and, therefore, rock fracture. For example, generally, corners tend to concentrate
771 stresses, and 'corner fractures' are a recognized phenomenon in fracture mechanics (e.g., Kobayashi and Enetanya, 1976). Thus,
772 this metric has been included as one to be measured both for outcrops and for clasts.

773

774 Sphericity refers to the length by width ratio, or elongation, of the clast or outcrop, whereas roundness is a measure of angularity
775 (Fig. 7). The roundness and sphericity designation for the square on the chart in Fig. 7 most closely matching the dominant shape
776 of the entire clast or outcrop should be noted (ex. r-SR; s-SE). If a more precise rock shape analysis is needed, a modified Kirkbride
777 device can be used to quantitatively measure rock roundness (see Cox et al., 2018 for device modifications and methodology).

778 ### 5.3.3 Grain size

779 Mean grain size can impact numerous fracture and stress characteristics including the proclivity for granular disintegration
780 (Gomez-Heras et al., 2006), fracture toughness (Zhang et al., 2018), initial fracture length, thermal stress disequilibrium (Janio De
781 Castro Lima and Paraguassú, 2004), and bulk elastic properties (Vazquez et al., 2015). The mean grain size is visually estimated
782 by comparing the dominant size of individual grains or mineral crystals to a standard grain size card. This size can be reported as
783 one average value for all minerals, or different values for different suites of minerals (e.g., felsic vs. mafic), depending on the
784 lithological assemblage(s) of the observation area(s) and the goals of the study.

785 ### 5.3.4 Fabric and fracture filling

786 Here, the term 'fabric' is employed to refer to any preexisting (prior to weathering) primary or diagenetic planar, linear, or randomly
787 oriented anisotropies within the rock comprising the outcrop or clast of interest. Fabric is most commonly observed as fossils or
788 lithological bedding planes in sedimentary rocks and as crystal horizons or foliation structures in igneous or metamorphic rocks.
789 Also, all rocks can have diagenetic mineral deposits within parts of otherwise open fractures or contain fully filled veins and dikes.
790 Finding mineral deposits in open fractures points to a deeper origin. Rock fabric can impart anisotropy that influences rock strength,
791 fluid flow, and fracturing clustering, rates, and orientations (e.g., Nara and Kaneko, 2006; Zhou et al., 2022). Thus, any visible
792 fabric type, as well as the strike(s) and dip(s) (or trend(s) and plunge(s)) of each parallel or subparallel set is noted in the fracture
793 sheet for each observation area. Through comparison of orientations, it can be determined the extent to which fractures in the
794 dataset are influenced by these fabrics.

795 ### 5.3.5 Fractures <2 cm in length

796 Fractures <2 cm in length can comprise a significant portion of all fractures on a given rock exposure, particularly in coarse
797 crystalline rock types (e.g., Alneasan and Behnia, 2021). Thus, it is recommended that an index is recorded (Sect. 5.2), using an
798 observation 'frame' that quantifies the abundance of fractures less than 2 cm in length (hereafter 'small fractures'). In our
799 experience, this data can help to explain, for example, fracture densities that are lower than expected when derived from the >2 cm
800 fracture length dataset alone.
801
802 The approximate number of small fractures visible each time the 'frame' is moved should be observed. A rough average of all
803 theoretical frames should be taken, and the categories in Fig. 5 should be used to assign an abundance. For example, if there are
804 generally either zero or one small fracture in any given 10 x 10 cm frame, the abundance would be "1" – i.e., few, <1 per unit area.

805 ### 5.3.6 Granular disintegration

806 Granular disintegration refers to evidence of *active* loss of individual crystals or grains due to fracturing along grain boundaries
807 (i.e., sedimentary particles or igneous or metamorphic crystals). This feature is observed on the rock surface as individual grains
808 or small clusters of grains of the rock that can be brushed away by hand. Granular disintegration is commonly observed in coarse
809 igneous, metamorphic, and sedimentary rocks, and over the long-term leads to the accumulation of 'grus' - sediment comprised of
810 individual crystals or small clusters of a few crystals on the ground surface (Eppes and Griffing, 2010; Isherwood and Street, 1976;
811 Gomez-Heras et al., 2006).
812

813   By necessity, this disintegration comprises the complete separation of intergranular fractures, and similar to fractures <2 cm, we

814   have experienced that it can provide information about smaller scale fracturing of the rock (e.g. Eppes et al., 2018). Because the

815   fractures that comprise granular disintegration are typically too small to be readily measured in the field, however, its presence is

816   assumed when loose grains are present on the rock surface. The worker marks affirmatively (circling the 'G' on the Fracture Sheet)

817   if there is evidence of granular disintegration on the rock surface of observation. If more detail is desired, an abundance index (e.g.,

818   Fig. 5) may be employed to quantify what percentage of the surface of observation contains loose grains.

5.3.7 Pitting

820   Pitting is the occurrence of small holes or fissures that form on the rock surface due to granular disintegration or to preferential

821   chemical weathering of certain mineral types, typically feldspars and micas in silicate rocks. Pitting is distinct from granular

822   disintegration as it is not necessarily 'actively' occurring – i.e., pitting can exist without loose grains on the rock surface. It is

823   included here as a rock property because of its possible linkage to intergranular fracturing. Furthermore, measuring the extent and

824   depth of pitting due to chemical weathering has long been employed as a relative age dating tool in Quaternary geology applications

825   (Burke and Birkeland, 1979).

827   Pitted surfaces form as individual grains become weathered and fall out or are dissolved; or, for soluble rocks like carbonates, as

828   entire rock regions are dissolved. Pitting is quantified either as present/absent (circling P on the fracture sheet) or as a quantity

829   index (Figs. 4 and 5).

5.3.8 Clast exposure

831   This metric is used to record to what degree individual clasts appear to be exposed above the ground surface. Individual clasts are

832   known to weather and erode from the upper rock surface down until they become 'flat' rocks at the ground surface (e.g. Ollier,

833   1984), and the degree if embeddedness can impact preservation of fracture orientations (e.g. Aldred et al., 2015). We have found

834   in our experience that surface exposure can be estimated as the amount and shape of a boulder's exposed surface that is currently

835   not covered by loose sediment, vegetation, or other material, and also relates to erosion rate in some settings. This exposure is

836   grouped into four categories: 0 - the clast is sitting above the ground, and its sides curve downward toward the ground surface

837   almost meeting; 1 - the clast is partially covered, with sides curving downward toward the ground surface but not meeting; 2 - the

838   clast is "half" covered, with sides projecting roughly vertically into the ground surface; 3 - the clast has only one upward facing

839   side visible at the ground surface. In a field study, a correlation test on data from 300 boulders revealed a positive correlation of

840   0.66 between the indices and the fraction of boulder embeddedness (in vertical height) (Shaanan et al., 2022).

5.3.9 Lichen and varnish

842   Lichens and other plant life can act to push rocks apart during growth (Scarciglia et al., 2012), but have also been shown to

843   strengthen rocks through infilling of voids or shielding from stress-inducing sunlight (Coombes et al., 2018). It is noted that lichen

844   are living organisms that would be killed by removal. We have found that in order to determine if a lichen-coated lineation is in

845   fact a measurable fracture (see Sect. 4.1), a large needle or straight pin may be employed to poke through the lichen into the

846   possible void of the fracture.

847

848 Rock varnish (oxide staining that can appear as a dark gray/black or orange coating on rock and typically contains Fe or Mn oxides)

849 is well-documented to evolve over time. The extent of varnish cover has been employed frequently as a relative-age indicator,

850 particularly in arid environments (e.g., Mcfadden and Hendricks, 1985; Macholdt et al., 2018). Thus, we infer that variations in

851 varnish across the rock face can provide evidence of loss of surface material through *in situ* fracturing.

852

853 Lichen and varnish can come in many forms and be difficult to distinguish from each other and from primary rock minerals, hiding

854 in fractures, pitting holes, and atop mafic crystals. So, careful consideration of the types of lichen and varnish that may be found

855 in field sites and close inspection with a hand lens is recommended. A fresher exposure of the rock surface can help in the

856 identification of lichen and varnish relative to the natural rock composition and color. Due to the geodiversity impact, however,

857 such exposures should not be made with force.

858

859 The quantity of lichen and varnish (secondary chemical precipitates deposited on the subaerial rock surface) visible on the rock

860 observation surface are separately estimated using a visual percentage estimator (Fig. 6) and a quantity index is assigned (Fig. 5;

861 Sect. 5.2).

862

863 **5.3.10 Collecting samples for microfracture analyses**

864 Rock microfractures (those not visible with hand lens in the field) play a central role in contributing to rock strength, anisotropy,

865 and subsequent macrofracturing processes (Kranz, 1983; Anders et al., 2014). It is beyond the scope of the field-based methods

866 presented herein to describe microfracture measurement and analysis, which continues to evolve (e.g., Griffiths et al., 2017; Healy

867 et al., 2017). Instead, suggestions for rock sampling and placement of thin-section billets are provided.

868

869 Thin-section analysis of microfractures can be a time-consuming process, particularly when considering the per-capita rock volume

870 examined. It is therefore extremely important to select rock or portions of rock that are precisely the rock type of interest, and to

871 carefully orient the sample. For loose clasts, an entire clast can be sampled and a thin-section billet processed in the lab. For larger

872 clasts and bedrock, a smaller portion must be extracted. By sampling pieces that are already naturally detached, or nearly detached,

873 fracturing that arises due to chiseling or hammering is avoided. Epoxying samples prior to thin section preparation helps preserve

874 delicate features and avoids introducing artifacts. Extra-thick sections are recommended for microfracture work, since conventional

875 sections are prone to develop fractures during grinding. For population sampling, continuous sections can be created of any length

876 (Gomez and Laubach, 2006).

877

878 For both clasts and outcrops, the natural orientation of the sampled rock (its horizontal and azimuthal directions) is always marked

879 on the specimen. The sample should be photographed prior to removing from its location. It is essential to ensure all permitting is

880 in place prior to sampling.

881

882 Similar to clast or outcrop selection, care must be taken when considering the location within the rock that the thin-section billet

883 will be cut. Because microfracture strike and dip can be influenced by environmental, gravitational, and tectonic forces, both the

884 depth and orientation of the billet should be noted and controlled for as appropriate for all samples compared within a single study.

885 5.3.11 Fracture connectivity

886 Fracture connectivity refers to the arrangement of fractures relative to each other and has long been recognized as being key to

887 rock strength and fluid flow (e.g., Rossen et al., 2000; Long and Witherspoon, 1985; Manzocchi, 2002; Viswanathan et al., 2022),

888 and presumably contributes to rock erodibility, given that fractures must intersect for rock to erode. There is a large body of

889 literature that addresses fracture connectivity and how to measure it (e.g., Berkowitz, 2002; Barton et al., 1993; Healy et al., 2017;

890 Sanderson and Nixon, 2018), especially in the context of reservoirs and rock quality index studies. As yet, fracture connectivity

891 has been little studied in the context of surface processes, but likely holds high potential given its relationship to water access and

892 to erodibility. Here, the focus is on a simple, rules-based observation of fracture intersection 'nodes' (e.g., Barton and Hsieh, 1989;

893 Manzocchi, 2002; Forstner and Laubach, 2022; Sanderson and Nixon, 2018) that comprise the basis for fracture network

894 connectivity assessment (e.g., Andresen et al., 2013).

895

896 After all fractures within each observation area have been identified and measured (Sect. 5.4), all fracture links within the

897 observation area should be counted and recorded by noting their relationship to other fractures (Fig. 8): dead end (I-node),

898 crossing (X-node), and/or abutting without crossing (Y-node). Numbers of nodes per area can then be used as a proxy for

899 fracture connectivity. If fracture connectivity is of particular interest for the research, rules-based 'contingent mode' (C-node)

900 intersections may also be added (Forstner and Laubach, 2022). An example of a C-node rule might be if fractures >100 mm in

901 length terminate within 10 mm of another fracture, its termination would be a c-node. Another C-node definition could comprise

902 intersection relations where visible connected traces are sealed with secondary minerals. These c-nodes may be important when

903 there are ambiguous at-depth relationships between fracture terminations (e.g., Fig. 2b).

904
905 5.3.12 Fracture spatial arrangement

906 In addition to overall fracture density, intensity and connectivity, the arrangement of fractures in space (e.g., evenly spaced,

907 random, clustered in space) can impact loci of rock mass weakness, fluid flow, and landscape morphology. Laubach et al. (2018)

908 comprises a special issue of the Journal of Structural Geology devoted to spatial arrangement of fractures, and much work has been

909 published since. The mathematical analysis of spatial arrangement and rigorous identification of clustering is beyond the scope of

910 this field guide. Freely available software is available for analyzing one-dimensional fracture arrangement along scan lines (Marrett

911 et al., 2018) and for analysis of trace patterns in two dimensions (Corrêa et al., 2022; Shakiba et al., 2022).

912

913 For scanline-based methods, following similar methods as those used for locating windows (Sect. 3.4), lines should be

914 established across representative parts, or the center, of each observation area. For 1D analysis, good practice is to establish at

915 least two perpendicular lines to capture different orientations of fractures, but the optimal number and configuration depends on

916 the pattern under investigation. A tape or other linear measuring tool is then arranged along the lines, and, beginning with the

917 edge of the observation area as distance 0, the distance along the tape of each fracture is noted (in other words, the sequence of

918 spacing between fractures is recorded), with each measurement linked to the "Crack ID" already established for that fracture on

919 the Fracture Sheet. If fractures are already marked with chalk, we find that this is an easy process. In that way, the size of each

920 fracture and its adjacent distances are noted (analysis procedures allow weighting by fracture height, length, or aperture). As with

921 any measure of fracture aggregate properties such as intensity or connectivity, for fractures having a wide range of sizes,

922 arrangement results depend on the size range of fractures included in the analysis (scale dependent) (e.g. Ortega et al., 2006).

923 These spatial arrangement data can go on the back of the Fracture Sheet.

924 **5.4 Individual fracture characteristics**

925 The following properties are measured for each fracture found within the observation area that meets all the fracture selection

926 criteria listed in Table 1. In order to keep track, we have found from experience that it is useful to mark fractures with chalk

927 within the observation area after you have made their appropriate measurements.

928 **5.4.1 Length**

929 Fracture length is measured for the entire surface exposure length of the fracture; i.e., around corners and up and down rock

930 topography (Fig. 2a). We have found these surface exposure distances to be the most repeatable and representative for the amount

931 of fracture exposed on the rock surface (Aldred et al., 2016). Measurements can be made with flexible seamstress tape to follow

932 the curve of a fracture's exposure on the rock surface. Length is only measured where there is an open void (Fig. 2b; Sect. 4.1),

933 because to measure across bridges of secondary cemented material or rock would be to infer future fracture propagation that has

934 not yet occurred. By only measuring the open portion of voids, the user avoids arbitrary interpretation of possible behavior. Thus,

935 if a seemingly continuous fracture (Fig. 2b, left inset) is in fact separated by bridges of solid rock (Fig. 2b, right inset), then these

936 should be measured as two different fractures and their lengths should terminate at the rock bridges (Sect. 4.1). The inset in Fig.

937 2b reveals four fractures possibly meeting all Table 1 criteria. If two fractures intersect in x- or y-nodes (Fig. 8), each fracture is

938 defined by its own distinct strike, and the full length of the full open fracture with that strike is measured (e.g., the length of

939 segments ab and cd in Fig. 8).

940

941 Importantly, when using a 'window' approach to rock observation area, both the total length of the fracture extending beyond the

942 window, as well as the total length within the window, should both be recorded. The latter is employed in fracture intensity

943 calculations (Sect. 6.1); the former provides representative information about all fracture lengths on the rock being measured.

944 **5.4.2 Width**

945 Fracture aperture widths (hereafter, 'widths') can impact both the strength and permeability of rock. Generally, they scale with

946 fracture length and, thus, can possibly reflect the innate subcritical cracking parameters of the rock (Olson, 2004). Fracture widths

947 typically vary along their exposure and pinch out at fracture tips. Determining an average or representative width within a single

948 fracture can thus be somewhat arbitrary and subject to bias. Locating the widest aperture is less subject to bias and can also provide

949 information about fracturing processes (for example, the widest aperture in a series of mechanically interacting en echelon fractures

950 should be in the center fracture; Anderson, 2005). Also, we find that the center of the open fracture is an objectively repeatable

951 location, and also where the fracture might be expected mechanistically to be the widest. However, given that this relationship can

952 become complicated as fractures fill or branch, unless there is reason to do otherwise, we recommend the rule of thumb to record

953 fracture width both at the midpoint of the measured length of the exposed fracture as well as at its maximum width along its

954 exposure.

955

956 We assert that in order to delineate the fracture – as opposed to measuring subsequent weathering or erosion - width measurements
957 should only be made in regions of the fracture where fracture walls are parallel or sub-parallel (e.g., green arrows in Fig. 9),
958 avoiding locations where fracture edges have been obviously rounded by erosion or chemical weathering, or where large pieces
959 have been chipped off or are missing (e.g., red arrows in Fig. 9). If it is unclear if a portion of the fracture has chipped off (e.g.,
960 orange arrow in Fig. 9), a notation can be made and employed later to eliminate potential outliers in the dataset. Fractures greater
961 than about 3 mm in width can be easily measured by inserting the back-blades of digital calipers into the widest opening of the
962 fracture. For narrower fractures, a logarithmically binned 'crack comparator' (Fig. 7) is recommended (Ortega et al., 2006),
963 whereby the line on the comparator most closely matching the fracture aperture is chosen.

964 **5.4.3 Strike and dip**

965 Fracture orientation (i.e., strike and dip) is a function of the orientation of existing anisotropy within the rock and the orientation
966 of the principal stresses that drove its propagation (e.g., Anderson, 2005). Fracture orientations are commonly related to tectonic
967 forces; however, both gravitational and environmental stresses can also be directional (e.g., St. Clair et al., 2015; Mcfadden et al.,
968 2005). When fractures are growing at subcritical rates, they can lengthen through a series of 'jumps' that link parallel or subparallel
969 smaller fractures (e.g., Ma et al., 2023). The following suggestions are for research aimed, not at characterizing these small mm-
970 cm scale heterogeneities, but rather identifying major stresses and heterogeneity in the entire rock body.
971

972 Fracture orientation is measured with a geological compass or similar tool that has both azimuthal direction and inclinometer
973 functionality. When measuring strike and dip of fractures, we find it is helpful to visualize how the fracture plane intersects the
974 rock surface, as if slipping a sheet of paper into the 'file folder' of the fracture. For larger fractures, weathering and erosion may
975 have resulted in loss of rock along the upper edge of the fracture, so it is imperative to measure the angle at the interior of the
976 fracture where its walls are parallel (Fig. 9) to avoid measuring instead the angle of the eroded face.
977

978 Fractures grow until they intersect other fractures and/or branch segment and link. If fractures appear to intersect, branch or link
979 (i.e., two connected planar voids with noticeably different orientations joined by a sharp angle), their lengths should be measured
980 separately as well as their orientations (e.g., two strikes and dips) as previously mentioned. This phenomenon is in some cases
981 evident in 2D spatial analysis that takes length scales into account (e.g., Corrêa et al., 2022). For fractures that meander around
982 mm-cm scale heterogeneities like phenocrysts or fossils, the overall trend is measured. A 1 to 10 rule of thumb (Sect. 4.1) can be
983 used whereby, as long as the 'jog' in the fracture orientation is <1/10 of the fracture length, it is not measured.
984

985 Fracture tip propagation direction may also slowly change as the orientation of external stresses or internal stress concentrations
986 change withing the rock mass. For curvilinear fractures, the average orientation can be measured, as the orientation of the non-
987 curved plane whose ends are defined by the ends of the fracture. Alternatively, the fracture curvilinear plane may be subdivided
988 into roughly linear planes and each orientation measured. If this latter approach is taken, the intersection should be marked as a
989 node, and two lengths recorded. It is important to note which method was employed and to remain consistent for all measurements,
990 as no widely acknowledged rule of thumb exists to our knowledge for this measurement.
991

992 There are numerous commonly-employed conventions for measurements of strike and dip. If the worker is consistent and clear in

993 the use of their preferred convention and in the presentation of their data, any are acceptable. If the worker has no such prior habits,

994 we recommend, from our experience, that to record strikes as an azimuthal orientation from 0-359 degrees, and dip angle as an

995 angle deviation from horizontal of 0-90 degrees makes data analysis easier than recording, for example, direction by quadrant. For

996 dip direction, we recommend a convention such as the "right-hand rule" be employed whereby the dip direction is always known

997 from the orientation of the strike alone. For example, the right-hand rule states that the down-dip direction is always to the "right"

998 of the measured and recorded strike when the observer is facing the same direction of the strike. Therefore, the strike that is

999 recorded is the one whereby the dip direction is always +90 degrees clockwise (to the right) from the strike direction.

1000 ### 5.4.4 Fracture parallelism

1001 Noting the parallelism of the fractures can help to better understand the origins of the population of fractures at a site. Parallelism

1002 is common because fractures often follow rock heterogeneities or anisotropies such as bedding, foliation, veins, or even the rock

1003 surface (e.g. McFadden et al., 2005). Fractures in a single bedrock outcrop or clast are also commonly parallel because they have

1004 formed due to external stress-loading with a consistent orientation (e.g., those influenced by regional tectonics or directional

1005 insolation). Thus, noting parallelism may help to distinguish the origins of fractures, though not always. For example, 'surface

1006 parallel fractures' (e.g., Fig. 2a) - commonly referred to as exfoliation, sheeting joints (e.g., Martel, 2017), or spalling – vary

1007 dramatically in scale and can have origins related to several different factors including tectonic-topographic interactions (Martel,

1008 2006), chemical weathering and volumetric expansion (Røyne et al., 2008), and thermal stresses related to insolation (e.g., Lamp

1009 et al., 2017; Collins and Stock, 2016) and fire (e.g., Buckman et al., 2021). Likewise, fractures having a strong preferred orientation

1010 parallel to topographic features like escarpments or stream channels may predate the topography and have localized the geomorphic

1011 feature, or they may postdate the feature and themselves be a response to topographic loads (e.g. Molnar, 2004). For this reason,

1012 fracture pattern sampling that seeks to avoid or characterize these effects should include exposures distant from such ambiguous

1013 situations (i.e., close to and distant from topographic features).

1014

1015 In the fracture sheet, features to which the fracture is parallel should be documented. We find that a visual inspection will suffice

1016 for most applications, but for applications where more precision is needed, the fracture may be considered parallel if the strike and

1017 dip of a fracture is within +/-10° of the orientation of the feature (the rock's long axis, its fabric, or its outer surface). We base this

1018 cutoff on the +/-4-7° strike and dip orientation precision of a typical Brunton compass under ideal measuring conditions (e.g.

1019 Whitmeyer et al., 2019). A fracture may be parallel to more than one feature in the rock. Categories may be added as necessary for

1020 rocks with other repeating features unique to the field site (fossils; veins, etc.). Assertions of parallelism (or similar) are a potential

1021 source of ambiguity, so careful consistency in the quantification of the basis of the claim is needed.

1022 ### 5.4.5 Sheet height

1023 Surface parallel fractures naturally detach 'sheets' of rock between the fracture and the rock surface ('h' in Fig. 2a). Sheet height

1024 is thus only measured for surface parallel fractures. We infer that the thickness of these sheets may be of interest for understanding

1025 the size of sediment produced from the fracture or for understanding the stresses that produced the fracture. We provide the rule

1026 of thumb that sheet height is measured using calipers at the location of the maximum height of the sheet, because thin edges often

1027 break off and vary. To limit these measurements to those that have likely formed in situ as related to the current morphology of

1028 the rock, another rule of thumb we have employed is to only measure those 'sheets' that would result in removal of <10% from

1029 the outer surface of the rock downward into the dimension(s) of the rock face(s) to which they are perpendicular.

1030 **5.4.6 Weathering index**

1031 Rock fracture is ultimately a molecular scale bond-breaking process; so, when fractures propagate, they initially form a razor-sharp

1032 lip or edge where their two planes intersect the rock surface. Over time, these edges naturally round through subsequent chemical

1033 and physical weathering, erosion, and abrasion (e.g., regions of the red arrows in Fig. 9). Crack tips may also blunt through time,

1034 but that observation may be complicated by the presence of mineral deposits. Following similar research that has demonstrated

1035 time-dependent changes in rock surface morphology due to such weathering processes (e.g., Shobe et al., 2017; Gómez-Pujol et

1036 al., 2006; McCarroll, 1991), we established an index of relative degree of such rounding along a fracture edge (rather than crack

1037 tip) to be noted in the fracture sheet:

1038
1039 1: fresh with evidence of recent rupture (flakes/pieces still present, but not attached)
1040 2: sharp, no rounded edges anywhere
1041 3: mostly sharp with occasional rounded edges
1042 4: mostly rounded edges with occasional sharp edges
1043 5: all rounded edges
1044

1045 **6 Suggestions for data analyses**

1046 When the data collection has been completed, it is necessary to provide statistics. For initial data exploration, general properties

1047 may be calculated for rock and fracture data like the mean, median, variance, skewness, kurtosis, and overall 'appearance' of

1048 distributions. Data can be compared using normal cross-plots, or quantile-quantile plots, as well as standard correlation analysis.

1049 For categorical data, normal analytical techniques (histograms, discrete correlation analysis, etc.) can be applied. As with all heavy-

1050 tailed data, the median is preferred over the mean value to understand a characteristic value—though power distributed data

1051 generally does not have a characteristic dimension. Distribution characterization is discussed in section 1.3. 2D spatial analysis

1052 methods can also be applied to entire outcrops or clasts, or to subdivisions of these features (Corrêa, et al., 2022: Shakiba et al.,

1053 2023). These methods are well suited to large outcrops and well exposed fracture arrays.

1054 **6.1 Fracture number density and fracture intensity**

1055 Here, following large portion of fracture mechanics literature and for clarity, the term 'fracture number density' is employed to

1056 refer to the number of fractures per unit area (e.g., # fractures/m^2), and the term 'fracture intensity' to the sum length of all fractures

1057 per unit area (e.g., cm/m^2). However, it is crucial to note that these terms are frequently defined differently and in inconsistent

1058 ways across disciplines and even within disciplines (e.g., Barthélémy et al., 2009; Narr and Lerche, 1984; Ortega et al., 2006;

1059 Dershowitz and Herda, 1992). To avoid confusion, it is imperative that workers clearly define their usage in each work. In

1060 particular, fracture intensity is scale dependent. If the outcrops or clasts on which fractures are measured vary greatly in size,

1061 intensity calculations that account for the fracture distribution may be appropriate (e.g. Ortega et al., 2006).

1062

1063 In the suggested simple use herein, the 'area' refers to the surface area of observation area. For fractures measured in 'windows'

1064 (Sect. 3.4), the length of fractures only *within* the window is used, and the area of the window (e.g., 10 cm x 10 cm) for the

1065 calculations. For loose clasts and outcrops, the appropriate calculation of surface area will depend on the shape and angularity of
1066 the rock. For most rocks, calculations for the surface area of the exposed sides of a rectangular cuboid (L*W + 2*(L*H) +
1067 2*(W*H)) are appropriate.

6.2 Circular data

1069 Standard 'linear' statistics cannot be employed for circular data. Instead, circular statistical and plotting software is used for the
1070 visualization and analysis of strike and dip data. The statistics employed by such software is typically based on established circular
1071 statistical research methods (e.g., Mardia and Jupp, 1972; Fisher, 1993). The following statistics are from that work and are useful
1072 in reporting strike and dip data.
1073
1074 The Mean Resultant Direction (a.k.a. vector mean, mean vector) is analogous to the slope in a linear regression. Circular variance
1075 can be quantified using either a Rayleigh Uniformity Test (for single mode datasets) or a Rao Spacing Test (for datasets with
1076 multiple modes), whereby p-values <0.05 indicate non-random orientations. If p-values for these tests are below a threshold (e.g.,
1077 <0.05), then data are considered non-uniform or non-random.
1078
1079 The Rayleigh statistic is based on a von Mises distribution (i.e., a normal distribution for circular data) of data about a single mean
1080 (i.e., unimodal data). Therefore, for multi-modal data, the variance might be high, but nevertheless, the data might be non-uniform.
1081 The Rayleigh Uniformity Test calculates the probability of the null hypothesis that the data are distributed in a uniform manner.
1082 Again, this test is based on statistical parameters that assume that the data are clustered about a single mean.
1083
1084 Rao's Spacing Test is also a test for the null hypothesis that the data are uniformly distributed; however, the Rao statistic examines
1085 the spacing between adjacent points to see if they are roughly equal (random with a spacing of 360/n) around the circle. Thus,
1086 Rao's Spacing Test is appropriate for multi-modal data and may find statistical significance where other tests do not.

8 Case example

1088 Here we present a simple, brief example of how the presented methods promote consistency of results across users in fracture
1089 measurements; to provide a full case study is beyond the scope of this paper. We provided minimal training (one demonstration
1090 with some minor oversight of initial work) to four groups of two students each. The fifth pair of workers included a scientist who
1091 had logged over 500+ hours of experience using the standardized methods. Each of the five groups followed the methods to
1092 measure the length and abundance of fractures on boulders (15-50 cm max diameter) on the same geomorphic surface (a 6000-
1093 year-old alluvial fan in Owens Valley California, comprised of primarily granitic rock types). Each group followed the methods
1094 described herein for rock and fracture selection and measurements. As such, the results from each group (Fig. 10; Data Supplement)
1095 could be compared not only for fracture selection and measurements, but also for observation area selection – a key component of
1096 collecting data that is representative of a particular site.
1097
1098 We find that the data collected by each of the groups for fracture length, number of fractures per rock, and rock size are statistically
1099 indistinguishable by student t-test (all pairs of p-values > 0.1; Fig. 10; Data Supplement). Also, there is no consistent difference
1100 between measurements made by the novice groups and that of the trained group. The mean fracture lengths from the four novice

groups novice group (37±23 mm to 59±51 mm) span across that of the mean collected by the well-trained group (42±22 mm; Supplement), as do the number of fractures per rock (2±2 to 6±8 for novice groups compared to 3±3 for trained group). With only one exception (fracture length for Group 1), variance between groups does not range by more than a factor of 3 in any of the data – a common rule of thumb for the threshold of 'similar' variance between small datasets. Overall, especially given the relatively small size of the datasets (~10-20 rocks and ~40-60 fractures each), this comparison suggests that the results using the standardized methods are reproducible, even with novice workers with minimal training. A full case study and analysis would be required to fully and quantitatively evaluate all of the procedures presented herein.

9 Conclusions

The methods proposed herein comprise a 'first stab' at standardization of field data collected in rock fracture research surrounding surface processes and weathering-based geologic problems. The outlined methods comprise best practices derived in large part from existing work in the context of structural geology and geotechnical engineering. They also comprise general guidance and nuances developed from experiences (and mistakes) over the last two decades of fracture-focused field research applied to geomorphology and soil science. We readily acknowledge that additional, fewer, or altered methods may be appropriate for some applications. Nevertheless, it is our hope that providing these rules-based, detailed, accessible, standardized procedures for gathering and reporting field-based fracture data will open the door to rapidly building a rigorous galaxy of new datasets as these guidelines and methods become more widely adopted. In turn, they may enable future workers to better compare and merge fracture data across a wide range of studies. Doing so will permit future refinements not only of the methods themselves, but most importantly of our understanding of rock fracture. Compiling such a standardized global dataset is the best hope for fully characterizing the role and nature of fractures in Earth surface systems and processes.

10 Author Contributions

MCE spearheaded the evolution of the development of the guiding principles and methods described herein as well as writing of the manuscript. AR and SL contributed significantly to the editing of the manuscript's content and expanding the breadth and depth of its applicability and approaches. JA, SB, MD, SE, FM, SP, MR, and US all participated extensively in field campaigns during which the methods were developed and refined, and they contributed to editing of manuscript and editing and development of figures. MM, AR and RK contributed to the development of theoretical statistical analyses practices that are outlined in the document and the editing of the manuscript.

11 Competing interests

The authors declare that they have no conflict of interest.

12 Data Availability

All data presented in the manuscript are available in the Supplement.

13 Acknowledgements

1134 The body of knowledge presented herein was derived in large part over the course of research funded by the National Science

1135 Foundation Grant Nos. EAR#0844335 (with supplements #844401, #0705277), #1744864, and NSF-BSF #1839148 and NASA

1136 ROSES Mars Data Analysis Program award #NNX09AI43G. Several photographs in figures were cropped and employed with

1137 permission from Marek Ranis, Artist-in-Residence for NSF #1744864. We thank Claire Bossennec and Colin Stark for their

1138 constructive reviews. In addition, the authors wish to acknowledge the contributions from countless undergraduate and graduate

1139 students who contributed to the application and development of these methods in classes taught by MCE at the University of North

1140 Carolina at Charlotte.

1141
1142
1143

Figure Captions

Fig. 1. Images illustrating the selection of observation areas for clasts and outcrops. A. Photograph of a transect established for clast selection. Black dot: predefined transect interval location on the tape. Red dot: clast that does not fit the predefined clast selection criteria (e.g., it is too big). Green dot with red circle: clast that fits criteria but is further away from the interval point that the clast with the green dot. Green dot: closest clast to the transect interval that meets the selection criteria. B. Annotated photograph showing an idealized placement of 'windows' (dashed black squares) on a bedrock outcrop. Outcrop dimensions are measured and the windows are placed using predetermined selection criteria. In this example, the windows are equally spaced along the centerline of the long-dimension of the upward-facing side of the outcrop.

Fig. 2. A. Example of the measurement of a surface exposure length (L; yellow line) of a fracture meeting the criteria in Table 1. The 'h' refers to the location where sheet height would be measured for this surface parallel fracture. B. Example of fractures that may appear to be a single fracture (left), but upon close examination are in fact multiple fractures intersecting and/or separated by rock (right inset). Arrow points to the location of the inset image on the main image. Compass in the foreground for scale.

Fig. 3. Example histograms and statistics of fracture length data measured on the exposed surfaces of clasts 15-50 cm max diameter. Upper row are data for clasts found on a modern ephemeral stream boulder bar. Clasts overall have very low fracture number density. Lower row are data for clasts on an ~6 ka surface where fracture number density is much higher. Note that it takes about 100 clasts to arrive at a statistically significant power law distribution for the Modern Wash clasts, but only 5 rocks for the rocks with higher fracture densities. Producing histograms interactively as data is collected can help establish how many observation areas are necessary for a given site.

Fig. 4. Reduced size image of an 8.5" x 11" 'fracture sheet' to be employed in the field to increase efficiency and to reduce 'missing' data. Sheet templates for both clasts and outcrops that can be modified are provided in Data Supplement as well as a data-entry template.

Fig. 5. Visual aid for estimating the abundance of "countable" rock features – including fractures. An index of 0-4 is assigned depending on the abundance of features within an average of any given observation area (ex: 10 x 10 cm) on the clast or window being examined. The area of observation is defined by the size of the features being measured. A 10 cm x 10 cm square is used for estimating the abundance of 'fractures < 2 cm' defined as fractures with lengths of >0.5 cm but < 2 cm (see section 5.2 for details of how to use the index). For features ≤0.5 cm, a 1 cm x 1 cm area would be employed and for features ≥2 cm, a 1 x 1 m area. Ensure the image is printed to scale prior to use in the field.

Fig. 6. A visual percent estimator (modified from Terry and Chilingar, 1955). Estimator should be employed in every estimate of percentages. See section 5.2 for using the estimator to assign a percent coverage index to features that are not countable or vary in size (e.g., lichen coverage, fine mafic minerals, etc.).

Fig. 7. **Inset:** Roundness and sphericity chart – modified from Krumbein and Sloss (1951) to add the roundness and sphericity lettering. **Roundness:** A = angular; SA = subangular; SR = subrounded; R = rounded; WR = well-rounded. **Sphericity:** S = spherical; SS = subspherical; SE = sub-elongate; E = elongate. **Edges:** fracture comparator whereby the width most closely matching the fracture aperture is noted. Note: a to-scale pdf is available in the Data Supplement, however, owing to printing and publication scaling, it is highly recommended to calibrate the comparator prior to using it in the field.

Fig. 8 Depiction of types of fracture intersection nodes. I-nodes comprise fracture terminations with no connections. Y-nodes are abutting fractures that do not cross. X-nodes are fractures that cross. C-nodes are 'contingent nodes' defined by the user. In this example the rule is related to the distance between I-nodes. For #1, the distance is wider than the criteria, so the terminations are designated as I-nodes. For #2, the distance is within the limits, and the 'connection' is designated as a C-node.

Fig. 9. Examples of aperture transects that are appropriate for measurement of fracture aperture widths (green) and transects where there is evidence that the fracture walls have been eroded or chipped and therefore should not be employed for a width

measurement (red). In cases where it is not clear if erosion or chipping has occurred (orange), a note can be made for the fracture width to possibly eliminate outliers during data analysis.

Fig. 10. Box and whisker plots of case example data collected by five different pairs of workers on the same geomorphic surface. "x"s mark the means. Groups 1-4 were novice workers. Group 5 comprised one experienced worker. A. Fracture lengths B. Fractures per rock C. Clast length

1202

1203 *Table 1. List of proposed rule-based criteria for defining measurable fractures*

The answer to the following questions must be 'yes' for all measured fractures. Measure all fractures meeting these criteria within the observation area.	NOTES
• Is the feature a lineament longer than it is wide? • Does the lineament contain open space bounded by walls? • If the lineament is not open, can the infilling material (ex: dust and lichens) be readily scraped out? • If the lineament is open or after the material has been scraped out, is the opening deeper than it is wide and bounded by ~parallel walls? • Is the open portion of the lineament ≥2 cm (>10 grains) in length (without interrupting bridges of rock or cemented infilling material)?	Do not measure: • Spherical pores/vesicles. • Lineaments, or portions of lineaments, with solid mineral infilling/cement. • Ledge edges or linear etchings. • rock bridges between fractures

1204

1205 *Table 2. List of proposed data to collect for the rock observation area and for all fractures ≥2 cm in length*

Rock Observations	Individual Fracture Observations
• Dimensions of the observation area (e.g. clast, outcrop, and/or window length, width, height) • Rock type • Grain size • Mineralogy % (minimally felsic vs. mafic) • Sphericity of exposure • Roundness of exposure • Fabric description, strike, and dip (e.g. vein, foliation, bedding) • Granular Disintegration • Pitting • Lichen and Varnish • Fracture Connectivity • Fracture Spacing	• Length (surface exposure length measured with a flexible tape) • Aperture width: center and maximum widths measured with calipers and/or comparator • Strike 0-360º (right-hand rule preferred) • Dip 0-90º • Parallelism (note features parallel to the fracture such as fabric, rock faces) • Sheet height (the thickness of what would be the detached spall or sheet of rock above a surface parallel fracture) • Weathering Index

1206
1207
1208
1209 *Table 3. List of field equipment*

Required	Recommended
• Hand lens (large, 10x) • Grain size card • Fracture comparator (for fracture widths) • Flexible seamstress tape measure (with mm) • Calipers (mm 0.0 to 150) • Brunton or similar compass • Roundness and sphericity chart • Visual percentage estimator • Fracture sheets	• Camera with macro lens • Chalk for marking measured fractures and windows • Safety pin or needle for fracture exploration • Cardboard cutout frames for windows • Small white board or chalk board for including observation area ID in photos

1210
1211

Bibliography

Aich, S. and Gross, M. R.: Geospatial analysis of the association between bedrock fractures and vegetation in an arid environment, International Journal of Remote Sensing, 29, 6937-6955, 10.1080/01431160802220185, 2008.

Al-Fahmi, M. M., Hooker, J. N., Al-Mojel, A. S., and Cartwright, J. A.: New scaling of fractures in a giant carbonate platform from outcrops and subsurface, Journal of Structural Geology, 140, 104142, https://doi.org/10.1016/j.jsg.2020.104142, 2020.

Aldred, J., Eppes, M. C., Aquino, K., Deal, R., Garbini, J., Swami, S., Tuttle, A., and Xanthos, G.: The influence of solar-induced thermal stresses on the mechanical weathering of rocks in humid mid-latitudes, Earth Surface Processes and Landforms, 41, 603-614, 2015.

Alneasan, M. and Behnia, M.: An experimental investigation on tensile fracturing of brittle rocks by considering the effect of grain size and mineralogical composition, International Journal of Rock Mechanics and Mining Sciences, 137, 104570, https://doi.org/10.1016/j.ijrmms.2020.104570, 2021.

Anderson, R. S.: Modeling the tor-dotted crests, bedrock edges, and parabolic profiles of high alpine surfaces of the Wind River Range, Wyomingc Geomorphology 46, 35-58, 2002.

Anderson, T. L.: Fracture Mechanics: Fundamentals and Applications, Third, Taylor & Francis Group, Boca Raton, FL, 2005.

Anders, M. H., Laubach, S. E., and Scholz, C. H., : Microfractures: a review. Journal of Structural Geology, 69, Part B, 377-394. doi: 10.1016/j.jsg.2014.05.011, 2014.

Andresen, C. A., Hansen, A., Le Goc, R., Davy, P., and Hope, S. M.: Topology of fracture networks, Frontiers in physics, 1, 7, 10.3389/fphy.2013.00007, 2013.

Andrews, B. J., Roberts, J. J., Shipton, Z. K., Bigi, S., Tartarello, M. C., and Johnson, G.: How do we see fractures? Quantifying subjective bias in fracture data collection, Solid Earth, 10, 487, 2019.

ASTM: D7012-14: Standard Test Methods for Compressive Strength and Elastic Moduli of Intact Rock Core Specimens Under Varying States of Stress and Temperatures, 2017.

Atkinson, B. K.: Fracture Mechanics of Rock, Academic Press Geology Series, Academic Press Inc., Orlando, Florida, https://doi.org/10.1016/C2009-0-21691-6, 1987.

Ayatollahi, M. R. and Akbardoost, J.: Size and geometry effects on rock fracture toughness: Mode I fracture, Rock Mechanics and Rock Engineering, 47, 677-687, 10.1007/s00603-013-0430-7, 2014.

Aydin, A. and Basu, A.: The Schmidt hammer in rock material characterization, Engineering Geology, 81, 1-14, https://doi.org/10.1016/j.enggeo.2005.06.006, 2005.

Baecher, G. B.: Statistical analysis of rock mass fracturing, Journal of the International Association for Mathematical Geology, 15, 329-348, 10.1007/BF01036074, 1983.

Balco, G.: Technical note: A prototype transparent-middle-layer data management and analysis infrastructure for cosmogenic-nuclide exposure dating, Geochronology, 2, 169-175, https://doi.org/10.5194/gchron-2-169-2020, 2020.

Barthélémy, J.-F., Guiton, M. L. E., and Daniel, J.-M.: Estimates of fracture density and uncertainties from well data, International Journal of Rock Mechanics and Mining Sciences, 46, 590-603, https://doi.org/10.1016/j.ijrmms.2008.08.003, 2009.

Barton, C. C. and Hsieh, P. A.: Physical and Hydrologic-Flow Properties of Fractures: Las Vegas, Nevada - Zion Canyon, Utah - Grand Canyon, Arizona - Yucca Mountain, Nevada, July 20-24, 1989 (Field Trip Guidebook T385), American Geophysical Union, Washington, D.C.1989.

Barton, C. C., Larsen, E., Page, W. R., and Howard, T. M.: Characterizing fractured rock for fluid-flow, geomechanical, and paleostress modeling: Methods and preliminary results from Yucca Mountain, Nevada, United States, Medium: ED; Size: 74 p., 10.2172/145208, 1993.

Bell, F.G.: Engineering Geology, 2nd ediction. Butterworth-Heinemann Press, Burlington, MA, USA. 581 p. ISBN 978-0-7506-8077-6. 2007.

Berberich, S.: A chronosequence of cracking in Mill Creek, California, Geography and Earth Sciences, The University of North Carolina Charlotte, ProQuest, 2020.

Berkowitz, B.: Characterizing flow and transport in fractured geological media: A review, Advances in Water Resources, 25, 861-884, https://doi.org/10.1016/S0309-1708(02)00042-8, 2002.

1258 Betlem, P., Birchall, T., Lord, G., Oldfield, S., Nakken, L., Ogata, K., and Senger, K.: High resolution digital outcrop model of
1259 faults and fractures in caprock shales, Konusdalen West, central Spitsbergen, Earth Syst. Sci. Data Discuss. [preprint],
1260 https://doi.org/10.5194/essd-2022-143, in review, 2022.

1261 Birkeland, P. W.: Soils and Geomorphology, Oxford University Press, New York, New York, 1999.

1262 Bonnet, E., Bour, O., Odling, N. E., Davy, P., Main, I., Cowie, P., and Berkowitz, B.: Scaling of fracture systems in geological
1263 media, Reviews of Geophysics, 39, 347-383, 2001.

1264 Borg, I. and Handin, J.: Experimental deformation of crystalline rocks, Tectonophysics, 3, 249-367, https://doi.org/10.1016/0040-
1265 1951(66)90019-9, 1966.

1266 Brantley, S. L., Eissenstat, D. M., Marshall, J. A., Godsey, S. E., Balogh-Brunstad, Z., Karwan, D. L., Papuga, S. A., Roering, J.,
1267 Dawson, T. E., Evaristo, J., Chadwick, O., McDonnell, J. J., and Weathers, K. C.: Reviews and syntheses: On the roles trees play
1268 in building and plumbing the critical zone, Biogeosciences, 14, 5115, 2017.

1269 Brantut, N., P. Baud, M. J. Heap, and Meredith, P. G.: Micromechanics of brittle creep in rocks, J. Geophys. Res. 117, B08412,
1270 doi:10.1029/2012JB009299, 2012.

1271 Brantut, N., Heap, M. J., Meredith, P. G., and Baud, P.: Time-dependent cracking and brittle creep in crustal rocks: A review,
1272 Journal of Structural Geology, 52, 17-43, 2013.

1273 Brilha, J., Gray, M., Pereira, D. I., and Pereira, P.: Geodiversity: An integrative review as a contribution to the sustainable
1274 management of the whole of nature, Environmental Science & Policy, 86, 19-28, https://doi.org/10.1016/j.envsci.2018.05.001,
1275 2018.

1276 Buckman, S., Morris, R. H., and Bourman, R. P.: Fire-induced rock spalling as a mechanism of weathering responsible for flared
1277 slope and inselberg development, Nature Communications, 12, 2150, 10.1038/s41467-021-22451-2, 2021.

1278 Burghelea, C., Zaharescu, D. G., Dontsova, K., Maier, R., Huxman, T., and Chorover, J.: Mineral nutrient mobilization by plants
1279 from rock: influence of rock type and arbuscular mycorrhiza, Biogeochemistry, 124, 187-203, 10.1007/s10533-015-0092-5, 2015.

1280 Burke, R. M. and Birkeland, P. W.: Reevaluation of multiparameter relative dating techniques and their application to the glacial
1281 sequence along the eastern escarpment of the Sierra Nevada, California, Quaternary Research, 11, 21-51, 10.1016/0033-
1282 5894(79)90068-1, 1979.

1283 Burnett, B. N., Meyer, G. A., and McFadden, L. D.: Aspect-related microclimatic influences on slope forms and processes,
1284 northeastern Arizona, Journal of Geophysical Research: Earth Surface, 113, https://doi.org/10.1029/2007JF000789, 2008.

1285 Buss, H. L., Sak, P. B., Webb, S. M., and Brantley, S. L.: Weathering of the Rio Blanco quartz diorite, Luquillo Mountains, Puerto
1286 Rico: Coupling oxidation, dissolution, and fracturing, Geochimica et Cosmochimica Acta, 72, 4488-4507, 2008.

1287 Chen, X., Eichhubl, P., and Olson, J. E.: Effect of water on critical and subcritical fracture properties of Woodford shale, Journal
1288 of Geophysical Research: Solid Earth, 122, 2736-2750, https://doi.org/10.1002/2016JB013708, 2017.

1289 Chilton, K. D. and Spotila, J. A.: Preservation of Valley and Ridge topography via delivery of resistant, ridge-sourced boulders to
1290 hillslopes and channels, Southern Appalachian Mountains, U.S.A, Geomorphology, 365, 107263,
1291 https://doi.org/10.1016/j.geomorph.2020.107263, 2020.

1292 Clauset, A., Shalizi, C. R., and Newman, M. E. J.: Power-law distributions in empirical data, SIAM review, 51, 661-703,
1293 10.1137/070710111, 2009.

1294 Collins, B. D. and Stock, G. M.: Rockfall triggering by cyclic thermal stressing of exfoliation fractures, Nature Geoscience, 9, 395-
1295 401, 2016.

1296 Coombes, M. A., Viles, H. A., and Zhang, H.: Thermal blanketing by ivy (*Hedera helix* L.) can protect building stone from
1297 damaging frosts, Nature: Scientific Reports, 8, 1-12, 2018.

1298 Corrêa, R. S. M., Marrett, R., and Laubach, S. E.: Analysis of spatial arrangement of fractures in two dimensions using point
1299 process statistics, Journal of Structural Geology, 163, 104726, https://doi.org/10.1016/j.jsg.2022.104726, 2022.

1300 Cox, R., Lopes, W. A., and Jahn, K. L.: Quantitative roundness analysis of coastal boulder deposits, Marine Geology, 396, 114-
1301 141, https://doi.org/10.1016/j.margeo.2017.03.003, 2018.

1302 Cuccuru, S., Casini, L., Oggiano, G., and Cherchi, G. P.: Can weathering improve the toughness of a fractured rock? A case study
1303 using the San Giacomo granite, Bulletin of Engineering Geology Environments, 71, 557-567, 2012.

D'Arcy, M., Roda Boluda, D. C., Whittaker, A. C. & Carpineti, A.: Dating alluvial fan surfaces in Owens Valley, California, using weathering fractures in boulders, Earth Surface Processes and Landforms 40, 487-501, 2014.

Davy, P., Le Goc, R., Darcel, C., Bour, O., de Dreuzy, J. R., and Munier, R.: A likely universal model of fracture scaling and its consequence for crustal hydromechanics, Journal of Geophysical Research: Solid Earth, 115, https://doi.org/10.1029/2009JB007043, 2010.

Deere, D.U.,:Technical descritpion of cores for engineering purposes. Rock Mechanics and Engineering Geology, 1, 18-22, 1964.

Dershowitz, W. S. and Herda, H. H.: Interpretation of fracture spacing and intensity, The 33rd U.S. Symposium on Rock Mechanics (USRMS), 1992.

DiBiase, R. A., Rossi, M. W., and Neely, A. B.: Fracture density and grain size controls on the relief structure of bedrock landscapes, Geology, 48, 399-402, 2018.

Domokos, G., Jerolmack, D. J., Kun, F., and Torok, J.: Plato's cube and the natural geometry of fragmentation, Proceedings of the National Academy of Sciences, 117, 18178-18185, 2020.

Dove, P. M.: Geochemical controls on the kinetics of quartz fracture at subcritical tensile stresses, Journal of Geophysical Research, 100, 349-359, 1995.

Engelder, T.: Stress Regimes in the Lithosphere, Princeton University Press, 1993.

Engelder, T.: Tectonic implications drawn from differences in the surface morphology on two joint sets in the Appalachian Valley and Ridge, Virginia, Geology, 32(5), 413-416, 2004.

English, J. M. and Laubach, S. E.: Opening-mode fracture systems: insights from recent fluid inclusion microthermometry studies of crack-seal fracture cements, Geological Society, London, Special Publications, 458, 257-272, doi:10.1144/SP458.1, 2017.

Eppes, M.-C., 2022. Mechanical Weathering: A Conceptual Overview. In: Shroder, J.J.F. (Ed.), Treatise on Geomorphology, vol. 3. Elsevier, Academic Press, pp. 30–45. https://dx.doi.org/10.1016/B978-0-12-818234- 5.00200-5.

Eppes, M. C. and Griffing, D.: Granular disintegration of marble in nature: A thermal-mechanical origin for a grus and corestone landscape, Geomorphology, 117, 170-180, 2010.

Eppes, M. C. and Keanini, R.: Mechanical weathering and rock erosion by climate-dependent subcritical cracking, Reviews of Geophysics, 55, 470-508, 2017.

Eppes, M. C., McFadden, L. D., Wegmann, K. W., and Scuderi, L. A.: Cracks in desert pavement rocks: Further insights into mechanical weathering by directional insolation, Geomorphology, 123, 97-108, 2010.

Eppes, M. C., Magi, B., Scheff, J., Warren, K., Ching, S., and Feng, T.: Warmer, wetter climates accelerate mechanical weathering in field data, independent of stress-loading, Geophysical Research Letters, 47, 1-11, 2020.

Eppes, M. C., Magi, B., Hallet, B., Delmelle, E., Mackenzie-Helnwein, P., Warren, K., and Swami, S.: Deciphering the role of solar-induced thermal stresses in rock weathering, GSA Bulletin, 128, 1315-1338, 2016.

Eppes, M. C., Hancock, G. S., Chen, X., Arey, J., Dewers, T., Huettenmoser, J., Kiessling, S., Moser, F., Tannu, N., Weiserbs, B., and Whitten, J.: Rates of subcritical cracking and long-term rock erosion, Geology, 46, 951-954, 2018.

Fisher, N. I.: Statistical Analysis of Circular Data, Cambridge University Press, Cambridge, England, https://doi.org/10.1017/CBO9780511564345, 1993.

Forstner, S. R. and Laubach, S. E.: Scale-dependent fracture networks, Journal of Structural Geology, 165, 104748, https://doi.org/10.1016/j.jsg.2022.104748, 2022.

Girard, L., Gruber, S., Weber, S., and Beutel, J.: Environmental controls of frost cracking revealed through in situ acoustic emission measurements in steep bedrock, Geophysical Research Letters, 40, 1748-1753, 10.1002/grl.50384, 2013.

Gischig, V. S., Moore, J. R., Evans, K. F., Amann, F., and Loew, S.: Thermomechanical forcing of deep rock slope deformation: 1. Conceptual study of a simplified slope, Journal of Geophysical Research, 116, 10.1029/2011JF002006, 2011.

Glade, R. C., Shobe, C. M., Anderson, R. S., and Tucker, G. E.: Canyon shape and erosion dynamics governed by channel-hillslope feedbacks, Geology, 47, 650-654, 10 .1130 /G46219.1, 2019.

Gomez, L. A., and Laubach, S. E.,: Rapid digital quantification of microfracture populations, Journal of Structural Geology, 28, 408-420, 2006.

1349 Gomez-Heras, M., Smith, B. J., and Fort, R.: Surface temperature differences between minerals in crystalline rocks: Implications
1350 for granular disaggregation of granites through thermal fatigue, Geomorphology, 78, 236-249, 2006.

1351 Gómez-Pujol, L., Fornós, J. J., and Swantesson, J. O. H.: Rock surface millimetre-scale roughness and weathering of supratidal
1352 Mallorcan carbonate coasts (Balearic Islands), Earth Surface Processes and Landforms, 31, 1792-1801,
1353 https://doi.org/10.1002/esp.1379, 2006.

1354 Griffiths, L., Heap, M. J., Baud, P., and Schmittbuhl, J.: Quantification of microcrack characteristics and implications for stiffness
1355 and strength of granite, International Journal of Rock Mechanics and Mining Sciences, 100, 138-150,
1356 https://doi.org/10.1016/j.ijrmms.2017.10.013, 2017.

1357 Hancock, G. S. and Kirwan, M.: Summit erosion rates deduced from 10Be: Implications for relief production in the central
1358 Appalachians, Geology, 35, 89-92, 10.1130/g23147a.1, 2007.

1359 Hancock, P. L.: Brittle microtectonics: Principles and practice, Journal of Structural Geology, 7, 437-457,
1360 https://doi.org/10.1016/0191-8141(85)90048-3, 1985.

1361 Handin, J. and Hager, R. V., Jr.: Experimental deformation of sedimentary rocks under confining pressure: Tests at room
1362 temperature on dry samples, AAPG Bulletin, 41, 1-50, 10.1306/5ceae5fb-16bb-11d7-8645000102c1865d, 1957.

1363 Handin, J. and Hager, R. V., Jr.: Experimental deformation of sedimentary rocks under confining pressure: Tests at high
1364 temperature, AAPG Bulletin, 42, 2892-2934, 10.1306/0bda5c27-16bd-11d7-8645000102c1865d, 1958.

1365 Handin, J., Hager Jr, R. V., Friedman, M., and Feather, J. N.: Experimental deformation of sedimentary rocks under confining
1366 pressure: Pore pressure tests, AAPG Bulletin, 47, 717-755, 1963.

1367 Hasenmueller, E. A., Gu, X., Weitzman, J. N., Adams, T. S., Stinchcomb, G. E., Eissenstat, D. M., Drohan, P. J., Brantley, S. L.,
1368 and Kaye, J. P.: Weathering of rock to regolith: The activity of deep roots in bedrock fractures, Geoderma, 300, 11-31,
1369 https://doi.org/10.1016/j.geoderma.2017.03.020, 2017.

1370 Hatır, M. E.: Determining the weathering classification of stone cultural heritage via the analytic hierarchy process and fuzzy
1371 inference system, Journal of Cultural Heritage, 44, 120-134, https://doi.org/10.1016/j.culher.2020.02.011, 2020.

1372 He, M., Xia, H., Jia, X., Gong, W., Zhao, F., and Liang, K.: Studies on classification, criteria, and control of rockbursts, Journal of
1373 Rock Mechanics and Geotechnical Engineering, 4, 97-114, 10.3724/SP.J.1235.2012.00097, 2012.

1374 Healy, D., Rizzo, R. E., Cornwell, D. G., Farrell, N. J. C., Watkins, H., Timms, N. E., Gomez-Rivas, E., and Smith, M.: FracPaQ:
1375 A MATLAB™ toolbox for the quantification of fracture patterns, Journal of Structural Geology, 95, 1-16,
1376 https://doi.org/10.1016/j.jsg.2016.12.003, 2017.

1377 Heard, H. C.: Effect of large changes in strain rate in the experimental deformation of Yule Marble, The Journal of Geology, 71,
1378 162-195, 1963.

1379 Hencher, S.: Practical Engineering Geology. Spon Press, New York, NY, USA. 450 p. ISBN 97800-203-89482-8. 2015.

1380 Hencher, S.: Practical Rock Mechanics. Spon Press, New York, NY, USA. 356 p. ISBN 978-1-4822-1726-1. 2019.

1381 Heidbach, O., Rajabi, M., Cui, X., Fuchs, K., Müller, B., Reinecker, J., Reiter, K., Tingay, M., Wenzel, F., Xie, F., Ziegler, M. O.,
1382 Zoback, M.-L., and Zoback, M.: The World Stress Map database release 2016: Crustal stress pattern across scales, Tectonophysics,
1383 744, 484-498, https://doi.org/10.1016/j.tecto.2018.07.007, 2018.

1384 Holder, J., Olson, J. E., and Philip, Z.: Experimental determination of subcritical crack growth parameters in sedimentary rock,
1385 Geophysical Research Letters, 28, 599-602, https://doi.org/10.1029/2000GL011918, 2001.

1386 Hooke, R.: Geomorphic evidence for Late-Wisconsin and Holocene tectonic deformation, Death Valley, California, GSA Bulletin,
1387 83, 2073-2098, 10.1130/0016-7606(1972)83[2073:Geflah]2.0.Co;2, 1972.

1388 Hooker, J. N., Laubach, S. E., and Marrett, R.: A universal power-law scaling exponent for fracture apertures in sandstones, GSA
1389 Bulletin, 126, 1340-1362, 10.1130/b30945.1, 2014.

1390 Hooker, J. N., Gale, J. F. W., Gomez, L. A., Laubach, S. E., Marrett, R., and Reed, R. M.: Aperture-size scaling variations in a
1391 low-strain opening-mode fracture set, Cozzette Sandstone, Colorado, Journal of Structural Geology, 31, 707-718,
1392 https://doi.org/10.1016/j.jsg.2009.04.001, 2009.

1393 Hooker, J.N., Laubach, S.E., and Marrett, R.,: Fracture-aperture size–frequency, spatial distribution, and growth processes in strata-
1394 bounded and non-strata-bounded fractures, Cambrian Mesón Group, NW Argentina, Journal of Structural Geology, 54, 54-71.
1395 doi.org/10.1016/j.jsg.2013.06.011, 2013.

1396 Isherwood, D. and Street, A.: Biotite-induced grussification of the Boulder Creek Granodiorite, Boulder County, Colorado, GSA
1397 Bulletin, 87, 366-370, 10.1130/0016-7606(1976)87<366:Bgotbc>2.0.Co;2, 1976.

1398 Janio de Castro Lima, J. and Paraguassú, A. B.: Linear thermal expansion of granitic rocks: influence of apparent porosity, grain
1399 size and quartz content, Bulletin of Engineering Geology and the Environment, 63, 215-220, 10.1007/s10064-004-0233-x, 2004.

1400 Jenny, H.: Factors of Soil Formation: A System of Quantitative Pedology, McGraw-Hill, New York, New York, 1941.

1401 Kobayashi, A. S. and Enetanya, A. N.: Stress intensity factor of a corner crack, Mechanics of Crack Growth, 1976.

1402 Kranz, R. L.: Microcrack in rocks: A review, Tectonophysics, 100, 449-480, 1983.

1403 Krumbein, W. C.: Fundamental attributes of sedimentary particles, University of Iowa Student Engineering Bulletin, 27, 318-331,
1404 1943.

1405 Krumbein, W. C. and Sloss, L. L.: Stratigraphy and Sedimentation, W. H. Freeman and Company, San Francisco, California, 1951.

1406 Lamp, J. L., Marchant, D. R., Mackay, S. L., and Head, J. W.: Thermal stress weathering and the spalling of Antarctic rocks,
1407 Journal of Geophysical Research: Earth Surface, 122, 3-24, https://doi.org/10.1002/2016JF003992, 2017.

1408 Laubach, S. E., Olson, J. E., and Gross, M. R.: Mechanical and fracture stratigraphy, AAPG Bulletin, 93, 1413-1426,
1409 10.1306/07270909094, 2009.

1410 Laubach, S. E., Lamarche, J., Gauthier, B. D. M., Dunne, W. M., and Sanderson, D. J.: Spatial arrangement of faults and opening-
1411 mode fractures, Journal of Structural Geology, 108, 2-15, https://doi.org/10.1016/j.jsg.2017.08.008, 2018.

1412 Laubach, S. E., Lander, R. H., Criscenti, L. J., Anovitz, L. M., Urai, J. L., Pollyea, R. M., Hooker, J. N., Narr, W., Evans, M. A.,
1413 Kerisit, S. N., Olson, J. E., Dewers, T., Fisher, D., Bodnar, R., Evans, B., Dove, P., Bonnell, L. M., Marder, M. P., and Pyrak-
1414 Nolte, L.: The role of chemistry in fracture pattern development and opportunities to advance interpretations of geological
1415 materials, Reviews of Geophysics, 57, 1065-1111, 10.1029/2019RG000671, 2019.

1416 Leith, K., Moore, J. R., Amann, F., and Loew, S.: In situ stress control on microcrack generation and macroscopic extensional
1417 fracture in exhuming bedrock, Journal of Geophysical Research, 119, 1-22, 2014.

1418 Leone, J. D., Holbrook, W. S., Reibe, C. S., Chorover, J., Ferre, T. P. A., Carr, B. J., and Callahan, R. P.: Strong slope-aspect
1419 control of regolith thickness by bedrock foliation, Earth Surface Processes and Landforms, 45, 2998-3010, 2020.

1420 Long, J., Jones, R., Daniels, S., Gilment, S., Oxlade, D., and Wilkinson, M.: Reducing uncertainty in fracture modelling: Assessing
1421 user bias in interpretations from satellite imagery, AAPG 2019 Annual Convention & Exhibition, San Antonio, TX, 2019.

1422 Long, J. C. S. and Witherspoon, P. A.: The relationship of the degree of interconnection to permeability in fracture networks,
1423 Journal of Geophysical Research: Solid Earth, 90, 3087-3098, https://doi.org/10.1029/JB090iB04p03087, 1985.

1424 Ma, J. et al. Comparison of subcritical crack growth and dynamic fracture propagation in rocks under double-torsion tests.
1425 International Journal of Rock Mechanics and Mining Sciences 170, 105481 (2023).

1426 Macholdt, D. S., Al-Amri, A. M., Tuffaha, H. T., Jochum, K. P., and Andreae, M. O.: Growth of desert varnish on petroglyphs
1427 from Jubbah and Shuwaymis, Ha'il region, Saudi Arabia, The Holocene, 28, 1495-1511, 10.1177/0959683618777075, 2018.

1428 Maffucci, R., Bigi, S., Corrado, S., Chiodi, A., Di Paolo, L., Giordano, G., and Invernizzi, C.: Quality assessment of reservoirs by
1429 means of outcrop data and "discrete fracture network" models: The case history of Rosario de La Frontera (NW Argentina)
1430 geothermal system, Tectonophysics, 647-648, 112-131, https://doi.org/10.1016/j.tecto.2015.02.016, 2015.

1431 Manzocchi, T.: The connectivity of two-dimensional networks of spatially correlated fractures, Water Resources Research, 38, 1-
1432 1-1-20, https://doi.org/10.1029/2000WR000180, 2002.

1433 Mardia, K. V. and Jupp, P. E.: Directional Statistics, Academic Press Inc., London, England, 1972.

1434 Marrett, R., Gale, J. F. W., Gómez, L. A., and Laubach, S. E.: Correlation analysis of fracture arrangement in space, Journal of
1435 Structural Geology, 108, 16-33, https://doi.org/10.1016/j.jsg.2017.06.012, 2018.

1436 Marshall, J., Clyne, J., Eppes, M. C., and Dawson, T.: Barking up the wrong tree? Tree root tapping, subcrtitical cracking, and
1437 potential influence on bedrock porosity, AGU 2021 Fall Abstracts, 2021a.

1438 Marshall, J. A., Roering, J. J., Rempel, A. W., Shafer, S. L., and Bartlein, P. J.: Extensive frost weathering across unglaciated
1439 North America during the Last Glacial Maximum, Geophysical Research Letters, 48, https://doi.org/10.1029/2020GL090305,
1440 2021b.

1441 Martel, S. J.: Effect of topographic curvature on near-surface stresses and application to sheeting joints, Geophysical Research
1442 Letters, 33, 2006.

1443 Martel, S. J.: Mechanics of curved surfaces, with application to surface-parallel cracks, Geophysical Research Letters, 38, 2011.

1444 Martel, S. J.: Progress in understanding sheeting joints over the past two centuries, Journal of Structural Geology, 94, 68-86, 2017.

1445 Matsuoka, N. and Murton, J.: Frost weathering: Recent advances and future directions, Permafrost and Periglacial Processes, 19,
1446 195-210, 10.1002/ppp.620, 2008.

1447 Matthews, J. A. and Winkler, S.: Schmidt-hammer exposure-age dating: A review of principles and practice, Earth-Science
1448 Reviews, 230, 104038, https://doi.org/10.1016/j.earscirev.2022.104038, 2022.

1449 McAuliffe, J. R., McFadden, L. D., Persico, L. P., and Rittenour, T. M.: Climate and vegetation change, hillslope soil erosion, and
1450 the complex nature of Late Quaternary environmental transitions, Eastern Mojave Desert, USA, Quaternary, 5, 43, 2022.

1451 McCarroll, D.: The Schmidt hammer, weathering, and rock surface roughness, Earth Surface Processes and Landforms, 16, 477-
1452 480, https://doi.org/10.1002/esp.3290160510, 1991.

1453 McFadden, L. D. and Hendricks, D. M.: Changes in the content and composition of pedogenic iron oxyhydroxides in a
1454 chronosequence of soils in southern California, Quaternary Research, 23, 189-204, https://doi.org/10.1016/0033-5894(85)90028-
1455 6, 1985.

1456 McFadden, L. D., Eppes, M. C., Gillespie, A. R., and Hallet, B.: Physical weathering in arid landscpaes due to diurnal variation in
1457 the direction of solar heating, GSA Bulletin, 117, 161-173, 2005.

1458 Mogi, K.: Effect of the intermediate principal stress on rock failure, Journal of Geophysical Research (1896-1977), 72, 5117-5131,
1459 https://doi.org/10.1029/JZ072i020p05117, 1967.

1460 Mogi, K.: Fracture and flow of rocks under high triaxial compression, Journal of Geophysical Research (1896-1977), 76, 1255-
1461 1269, https://doi.org/10.1029/JB076i005p01255, 1971.

1462 Molaro, J. L., Byrne, S., and Le, J.-L.: Thermally induced stresses in boulders on airless body surfaces, and implications for rock
1463 breakdown, Icarus, 294, 247-261, 2017.

1464 Molaro, J. L., Hergenrother, C. W., Chesley, S. R., Walsh, K. J., Hanna, R. D., Haberle, C. W., Schwartz, S. R., Ballouz, R.-L.,
1465 Bottke, W. F., Campins, H. J., and Lauretta, D. S.: Thermal fatigue as a driving mechanism for activity on asteroid Bennu, Journal
1466 of Geophysical Research, 125, 1-24, 10.1029/2019JE006325, 2020.

1467 Molnar, P.: Interactions among topographically induced elastic stress, static fatigue, and valley incision, Journal of Geophysical
1468 Research, 109, 1-9, 10.1029/2003JF000097, 2004.

1469 Moon, S., Perron, J. T., Martel, S. J., Goodfellow, B. W., Ivars, D. M., Hall, A., Heyman, J., Munier, R., Naslund, J., Simeonov,
1470 A., and Stroeven, A. P.: Present-day stress field influences bedrock fracture openness deep into the subsurface, Geophysical
1471 Research Letters, 47, 1-10, 2020.

1472 Moon, S., Perron, J. T., Martel, S. J., Goodfellow, B. W., Mas Ivars, D., Simeonov, A., Munier, R., Naslund, J.-O., Hall, A.,
1473 Stroeven, A. P., Ebert, K., and Heyman, J.: Landscape features influence bedrock fracture openness in the deep subsurface,
1474 Geological Society of American Annual Meeting, Phoenix, AZ, USA, 10.1130/abs/2019AM-336309,

1475 Moser, F.: Spatial and temporal variance in rock dome exfoliation and weathering near Twain Harte, California, USA, Geography
1476 and Earth Sciences, The University of North Carolina Charlotte, ProQuest, 2017.

1477 Mushkin, A., Sagy, A., Trabelci, E., Amit, R., and Porat, N.: Measure the time and scale-dependency of subaerial rock weathering
1478 rates over geologic time scales with ground-based lidar, Geology, 42, 1063-1066, 2014.

1479 Nara, Y. and Kaneko, K.: Sub-critical crack growth in anisotropic rock, International Journal of Rock Mechanics and Mining
1480 Sciences, 43, 437-453, https://doi.org/10.1016/j.ijrmms.2005.07.008, 2006.

1481 Nara, Y., Kashiwaya, K., Nishida, Y., and Ii, T.: Influence of surrounding environment on subcritical crack growth in marble,
1482 Tectonophysics, 706-707, 116-128, 2017.

1483 Nara, Y., Morimoto, K., Hiroyoshi, N., Yoneda, T., Kaneko, K., and Benson, P. M.: Influence of relative humidity on fracture
1484 toughness of rock: Implications for subcritical crack growth, International Journal of Solids and Structures, 49, 2471-2481,
1485 https://doi.org/10.1016/j.ijsolstr.2012.05.009, 2012.

1486 Narr, W. and Lerche, I.: A method for estimating subsurface fracture density in core, AAPG Bulletin, 68, 637-648,
1487 10.1306/ad461354-16f7-11d7-8645000102c1865d, 1984.

1488 Neely, A. B., DiBiase, R. A., Corbett, L. B., Bierman, P. R., and Caffee, M. W.: Bedrock fracture density controls on hillslope
1489 erodibility in steep, rocky landscapes with patchy soil cover, southern California, USA, Earth and Planetary Science Letters, 522,
1490 186-197, https://doi.org/10.1016/j.epsl.2019.06.011, 2019.

1491 Ollier, C. D.: Weathering, 2nd, Longman, London, England, 1984.

1492 Olsen, T., Borella, J., and Stahl, T.: Clast transport history influences Schmidt hammer rebound values, Earth Surface Processes
1493 and Landforms, 45, 1392-1400, https://doi.org/10.1002/esp.4809, 2020.

1494 Olson, J. E.: Predicting fracture swarms - the influence of subcritical crack growth and the crack-tip process zone on joint spacing
1495 in rock, Geological Society of London Special Publications, 231, 73-87, 2004.

1496 Ortega, O. and Marrett, R.: Prediction of macrofracture properties using microfracture information, Mesaverde Group sandstones,
1497 San Juan basin, New Mexico, Journal of Structural Geology, 22, 571-588, https://doi.org/10.1016/S0191-8141(99)00186-8, 2000.

1498 Ortega, O. J., Marrett, R. A., and Laubach, S. E.: A scale-independent approach to fracture intensity and average spacing
1499 measurement, AAPG Bulletin, 90, 193-208, 10.1306/08250505059, 2006.

1500 Paris, P. and Erdogan, F.: A critical analysis of crack propagation laws, Journal of Basic Engineering, 85, 528-533,
1501 10.1115/1.3656900, 1963.

1502 Phillips, J. D.: An evaluation of the factors determining the effectiveness of water quality buffer zones, Journal of Hydrology, 107,
1503 133-145, https://doi.org/10.1016/0022-1694(89)90054-1, 1989.

1504 Ponti, S., Pezza, M., and Guglielmin, M.: The development of Antarctic tafoni: Relations between differential weathering rates
1505 and spatial distribution of thermal events, salts concentration, and mineralogy, Geomorphology, 373, 2021.

1506 Ramcharan, A., Hengl, T., Nauman, T., Brungard, C., Waltman, S., Wills, S., and Thompson, J.: Soil property and class maps of
1507 the conterminous United States at 100-meter spatial resolution, Soil Science Society of America Journal, 82, 186-201,
1508 https://doi.org/10.2136/sssaj2017.04.0122, 2018.

1509 Ramulu, M., Chakraborty, A. K., and Sitharam, T. G.: Damage assessment of basaltic rock mass due to repeated blasting in a
1510 railway tunnelling project – A case study, Tunnelling and Underground Space Technology, 24, 208-221,
1511 https://doi.org/10.1016/j.tust.2008.08.002, 2009.

1512 Rasmussen, M., Eppes, M. C., and Berberich, S.: Untangling the impacts of climate, lithology, and time on rock cracking rates and
1513 morphology in arid and semi-arid Eastern California, AGU Fall Meeting, New Orleans, LA, 2021.

1514 Ravaji, B., Ali-Lagoa, V., Delbo, M., and Wilkerson, J. W.: Unraveling the mechanics of thermal stress weathering rate-effects,
1515 size-effects, and scaling laws., Journal of Geophysical Research, 121, 3304-3328, 10.1029/2019JE006019, 2019.

1516 Riebe, C. S., Callahan, R. P., Granke, S. B.-M., Carr, B. J., Hayes, J. L., Schell, M. S., and Sklar, L. S.: Anisovolumetric weathering
1517 in granitic saprolite controlled by climate and erosion rate, Geology, 1-5, 10.1130/G48191.1, 2021.

1518 Rossen, W. R., Gu, Y., and Lake, L. W.: Connectivity and permeability in fracture networks obeying power-law statistics, SPE
1519 Permian Basin Oil and Gas Recovery Conference, 10.2118/59720-ms, 2000.

1520 Røyne, A., Jamtveit, B., Mathiesen, J., and Malthe-Sørenssen, A.: Controls on rock weathering rates by reaction-induced
1521 hierarchical fracturing, Earth and Planetary Science Letters, 275, 364-369, https://doi.org/10.1016/j.epsl.2008.08.035, 2008.Rysak,
1522 B., Gale, J. F., Laubach, S. E., & Ferrill, D. A.: Mechanisms for the generation of complex fracture networks: Observations from
1523 slant core, analog models, and outcrop, Frontiers in Earth Science, 10, 848012, 2022.

1524 Sanderson, D. J.: Field-based structural studies as analogues to sub-surface reservoirs, Geological Society, London, Special
1525 Publications, 436, 207-217, doi:10.1144/SP436.5, 2016.

1526 Sanderson, D. J. and Nixon, C. W.: Topology, connectivity and percolation in fracture networks, Journal of Structural Geology,
1527 115, 167-177, https://doi.org/10.1016/j.jsg.2018.07.011, 2018.

1528 Scarciglia, F., Saporito, N., La Russa, M. F., Le Pera, E., Macchione, M., Puntillo, D., Crisci, G. M., and Pezzino, A.: Role of
1529 lichens in weathering of granodiroite in the Sila uplands (Calabria, Southern Italy), Sedimentary Geology, 280, 119-134, 2012.

1530 Schoeneberger, P. J., Wysocki, D. A., and Benham, E. C.: Field Book for Describing and Sampling Soils: Version 3.0, Natural
1531 Resources Conservation Service, National Soil Survey Center, Lincoln, Nebraska2012.

Schultz, R. A.: Geologic Fracture Mechanics, Cambridge University Press, Cambridge, England, DOI: 10.1017/9781316996737, 2019.

Shakiba, M., Lake, L.W., Gale, J.F.W., Laubach, S.E., Pyrcz, M.J.: Multiscale spatial analysis of fracture nodes in two dimensions, Marine & Petroleum Geology, 149, 106093, doi.org/10.1016/j.marpetgeo.2022.106093, 2023.

Sharifigaliuk, H., Mahmood, S. M., Ahmad, M., and Rezaee, R.: Use of outcrop as substitute for subsurface shale: Current understanding of similarities, discrepancies, and associated challenges, Energy & Fuels, 35, 9151-9164, 10.1021/acs.energyfuels.1c00598, 2021.

Shi, J.: Study of thermal stresses in rocks due to diurnal solar exposure, Civil Engineering, University of Washington, 58 pp., 2011.

Shobe, C. M., Hancock, G. S., Eppes, M. C., and Small, E. E.: Field evidence for the influence of weathering on rock erodibility and channel form in bedrock rivers, Earth Surface Processes and Landforms, 42, 1997-2012, 2017.

Sklar, L. S., Riebe, C. S., Marshall, J. A., Genetti, J., Leclere, S., Lukens, C. L., and Merces, V.: The problem of predicting the size distribution of sediment supplied by hillslopes to rivers, Geomorphology, 277, 31-49, 2017.

Snowdon, A. P., Normani, S. D., and Sykes, J. F.: Analysis of crystalline rock permeability versus depth in a Canadian Precambrian rock setting, Journal of Geophysical Research: Solid Earth, 126, e2020JB020998, https://doi.org/10.1029/2020JB020998, 2021.

Sousa, L. M. O.: Evaluation of joints in granitic outcrops for dimension stone exploitation, Quarterly Journal of Engineering Geology and Hydrogeology, 43, 85-94, 10.1144/1470-9236/08-076, 2010.

St. Clair, J., Moon, S., Holbrook, W. S., Perron, J. T., Riebe, C. S., Martel, S. J., Carr, B., Harman, C., Singha, K., and Richter, D. D.: Geophysical imaging reveals topographic stress control of bedrock weathering, Geomorphology, 350, 534-538, 2015.

Staff, Soil Survey: Soil Taxonomy: A basic system of soil classification for making and interpreting soil surveys, 1999.

R.D. Terzaghi: Sources of error in joint surveys, Geotechnique, 15, 287-304, 1965.

Terry, R. D. and Chilingar, G. V.: Summary of "Concerning some additional aids in studying sedimentary formations," by M. S. Shvetsov, Journal of Sedimentary Research, 25, 229-234, 10.1306/74d70466-2b21-11d7-8648000102c1865d, 1955.

Turner, F. J., Griggs, D. T., and Heard, H. C.: Experimental deformation of calcite crystals, GSA Bulletin, 65, 883-934, 10.1130/0016-7606(1954)65[883:Edocc]2.0.Co;2, 1954.

Ukar, E., Laubach, S. E., and Hooker, J. N.: Outcrops as guides to subsurface natural fractures: Example from the Nikanassin Formation tight-gas sandstone, Grande Cache, Alberta foothills, Canada, Marine and Petroleum Geology, 103, 255-275, https://doi.org/10.1016/j.marpetgeo.2019.01.039, 2019.

Ulusay, R. and Hudson, J. A.: The Complete ISRM Suggested Methods for Rock Characterization, Testing and Monitoring: 1974-2006, Commission on Testing Methods, International Society of Rock Mechanics., Ankara, Turkey2007.

Ulusay, R (ed.), 2015. The ISRM suggested methods for rock characterization, testing and monitoring: 2007–2014. Springer, Cham, Switzerland. DOI:10.1007/978-3-319-007713-0."Vazquez, P., Shushakova, V., and Gomez-Heras, M.: Influence of mineralogy on granite decay induced by temperature increase: Experimental observations and stress simulation, Engineering Geology, 189, 58-67, 2015.

Viswanathan, H.S., et al: From fluid flow to coupled processes in fractured rock: recent advances and new frontiers, Reviews of Geophysics, 60(1), e2021RG000744, 2022.

Wang, H. F., Bonner, B. P., Carlson, S. R., Kowallis, B. J., and Heard, H. C.: Thermal stress cracking in granite, Journal of Geophysical Research: Solid Earth, 94, 1745-1758, https://doi.org/10.1029/JB094iB02p01745, 1989.

Wang, Q., Narr, W., Laubach, S.E.,: Quantitative characterization of fracture spatial arrangement and intensity in a reservoir anticline using horizontal wellbore image logs and an outcrop analog, Marine & Petroleum Geology, 152, 106238, https://doi.org/10.1016/j.marpetgeo.2023.106238, 2023.

Watkins, H., Bond, C. E., Healy, D., and Butler, R. W. H.: Appraisal of fracture sampling methods and a new workflow to characterise heterogeneous fracture networks at outcrop, Journal of Structural Geology, 72, 67-82, https://doi.org/10.1016/j.jsg.2015.02.001, 2015.

Weiserbs, B. I.: The morphology and history of exfoliation on rock domes in the Southeastern United States, Geography and Earth Sciences, The University of North Carolina Charlotte, ProQuest, 2017.

1577 Weiss, M.: Techniques for estimating fracture size: A comparison of methods, International Journal of Rock Mechanics and Mining
1578 Sciences, 45, 460-466, https://doi.org/10.1016/j.ijrmms.2007.07.010, 2008.

1579 Wenk, H.-R.: Some roots of experimental rock deformation, Bulletin de Mineralogie, 102, 195-202,
1580 https://doi.org/10.3406/bulmi.1979.7277, 1979.

1581 West, N., Kirby, E., Bierman, P. R., and Clarke, B. A.: Aspect-dependent variations in regolith creep revealed by meteoric 10Be,
1582 Geology, 42, 507-510, 10.1130/g35357.1, 2014.

1583 Whitmeyer, S., Pyle, E., Pavlis, T., Swanger, W. & Roberts, L.: Modern approaches to field data collection and mapping: Digital
1584 methods, crowdsourcing, and the future of statistical analyses, Journal of Structural Geology, 125, 29-40, 2019.

1585 Wohl, E. E.: The effect of bedrock jointing on the formation of straths in the Cache la Poudre River drainage, Colorado Front
1586 Range, Journal of Geophysical Research: Earth Surface, 113, https://doi.org/10.1029/2007JF000817, 2008.

1587 Wolman, M. G.: A method of sampling coarse river-bed material, Eos, Transactions American Geophysical Union, 35, 951-956,
1588 https://doi.org/10.1029/TR035i006p00951, 1954.

1589 Wu, H. and Pollard, D. D.: An experimental study of the relationship between joint spacing and layer thickness, Journal of
1590 Structural Geology, 17, 887-905, https://doi.org/10.1016/0191-8141(94)00099-L, 1995.

1591 Zeeb, C., Gomez-Rivas, E., Bons, P. D., and Blum, P.: Evaluation of sampling methods for fracture network characterization using
1592 outcrops, AAPG Bulletin, 97, 1545-1566, 10.1306/02131312042, 2013.

1593 Zeng, Fan, Biao Shu, and Qiwu Shen. "A combination of Light Detection and Ranging with Digital Panoramic Borehole Camera
1594 System in fracture mapping to characterize discrete fracture networks." Bulletin of Engineering Geology and the Environment 82,
1595 no. 7, 249, https://doi.org/10.1007/s10064-023-03274-5 , 2023:

1596 Zhang, C., Hu, X., Wu, Z., and Li, Q.: Influence of grain size on granite strength and toughness with reliability specified by normal
1597 distribution, Theoretical and Applied Fracture Mechanics, 96, 534-544, https://doi.org/10.1016/j.tafmec.2018.07.001, 2018.

1598 Zhang, L.: Determination and applications of rock quality designation (RQD), Journal of Rock Mechanics and Geotechnical
1599 Engineering, 8, 389-397, https://doi.org/10.1016/j.jrmge.2015.11.008, 2016.

1600 Zhou, W., Shi, G., Wang, J., Liu, J., Xu, N., and Liu, P.: The influence of bedding planes on tensile fracture propagation in shale
1601 and tight sandstone, Rock Mechanics and Rock Engineering, 55, 1111-1124, 10.1007/s00603-021-02742-2, 2022.

1602

FIGURE 1

Fig. 3

FIGURE 4

Name(s) & Date:
Site Name:
GPS Cooridnates:
GPS Projection:
Orientation conventions:
Declination:
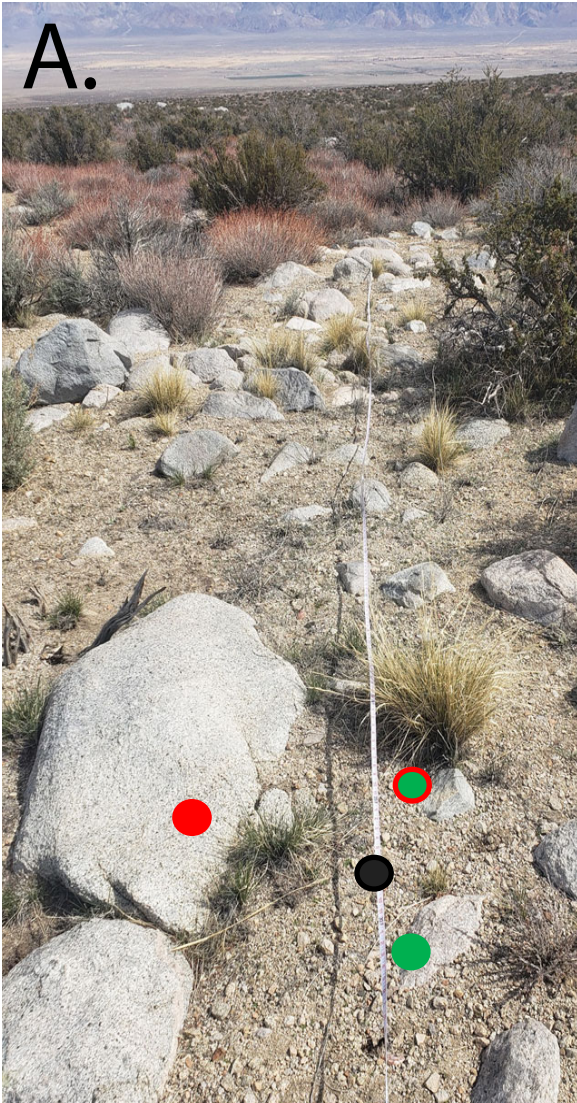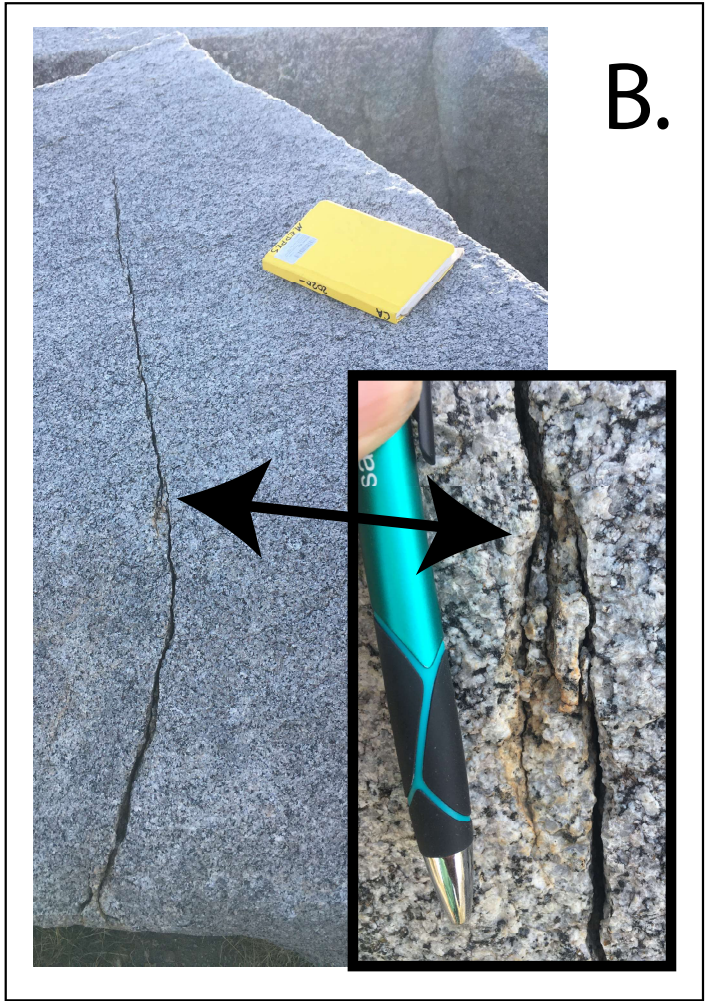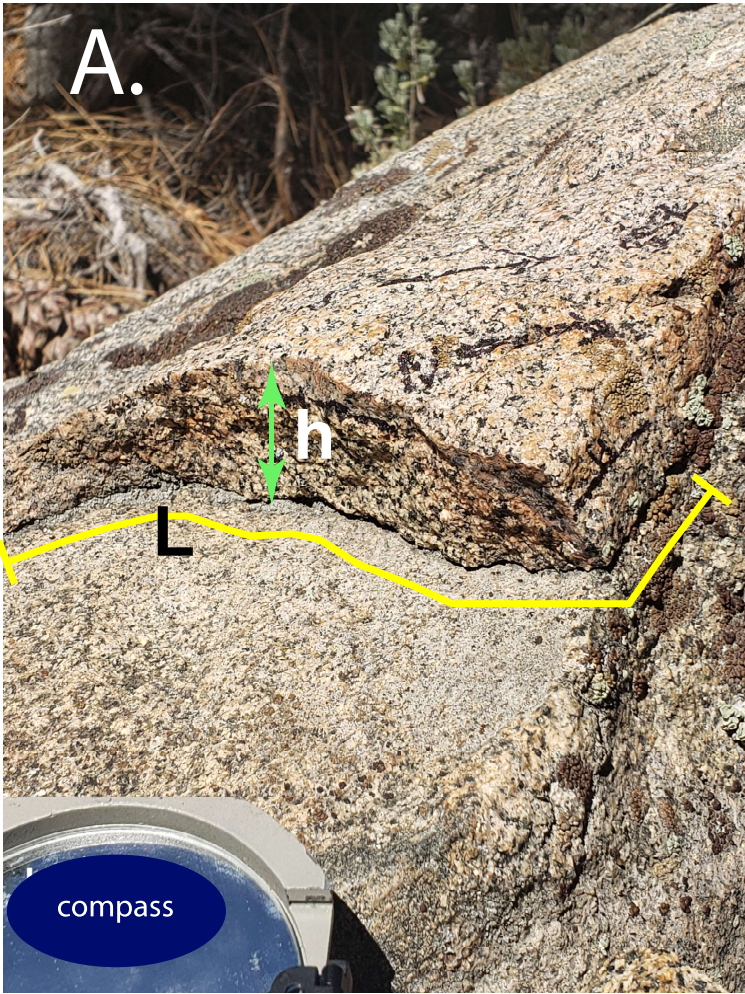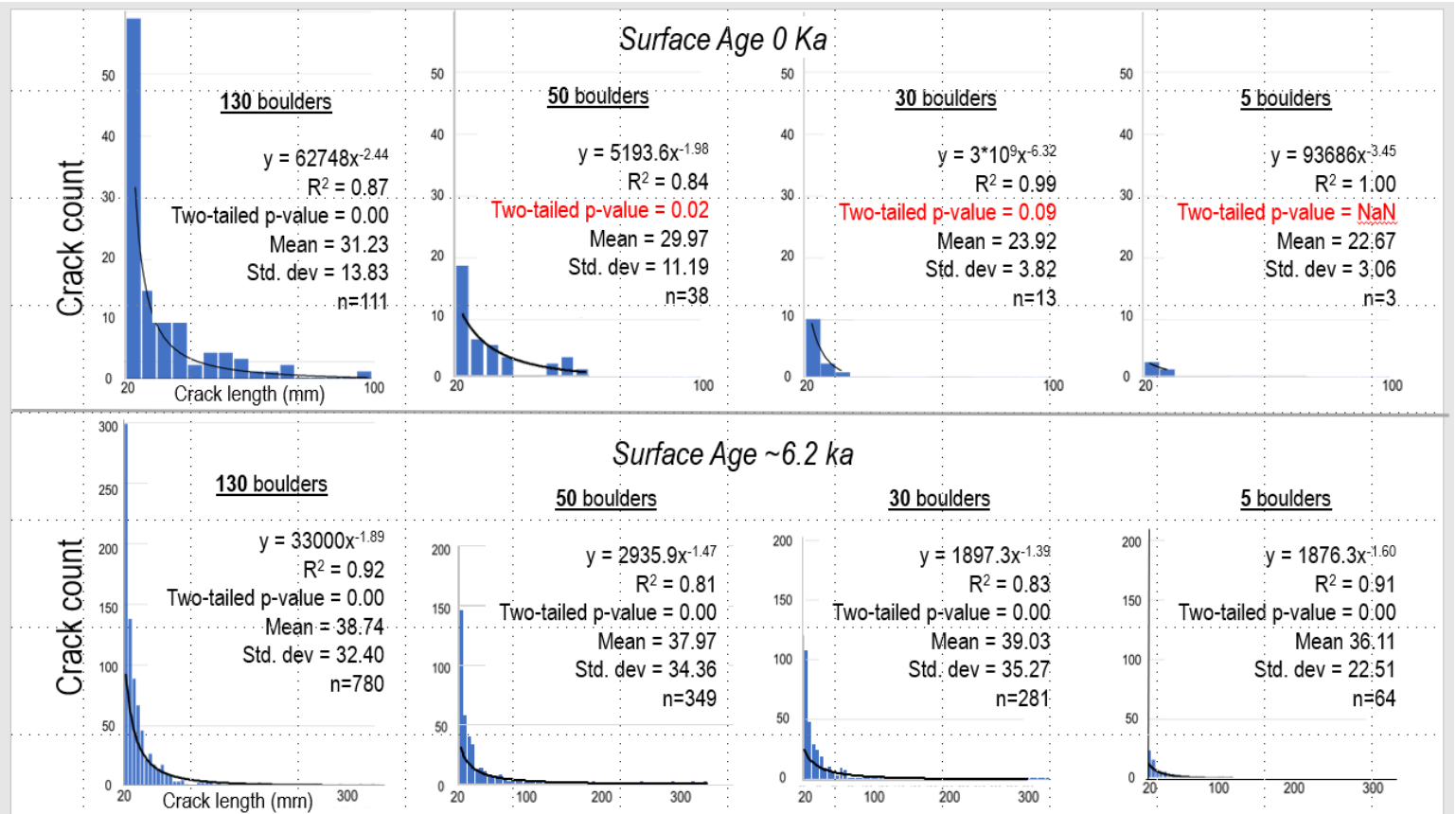
Criteria for Clast/Outcrop selection:
Portion observed (eg. All exposed, north face only, etc.):

Relevant Cl, O, R, P, T,T observations:
Vegetation-type & percent of each:
open ground cover (%):
Surface Slope:
Other:

ID & Rock Type	Avg. Grain Size (mm)	spheri-city/round-ness	Minerology	Length (cm)	Width (cm)	Height (cm)	Exposure	Cracks <2 cm	GD & Pit	Lichen	Varnish	Fabric Type	Fabric Strike (°)	Fabric Dip (°)	Crack ID	Crack Parallel to	Mid Crack Width (mm)	Crack Max Width (mm)	Crack Length (mm)	Crack Strike (°)	Crack Dip (°)	Sheet Ht. (mm)	Weathering Index	Notes
		s- r-					0123	012345	g p	012345	012345	F S B V O				S F L							1 2 3 4 5	
		s- r-					0123	012345	g p	012345	012345	F S B V O				S F L							1 2 3 4 5	
		s- r-					0123	012345	g p	012345	012345	F S B V O				S F L							1 2 3 4 5	
		s- r-					0123	012345	g p	012345	012345	F S B V O				S F L							1 2 3 4 5	
		s- r-					0123	012345	g p	012345	012345	F S B V O				S F L							1 2 3 4 5	
		s- r-					0123	012345	g p	012345	012345	F S B V O				S F L							1 2 3 4 5	
		s- r-					0123	012345	g p	012345	012345	F S B V O				S F L							1 2 3 4 5	
		s- r-					0123	012345	g p	012345	012345	F S B V O				S F L							1 2 3 4 5	
		s- r-					0123	012345	g p	012345	012345	F S B V O				S F L							1 2 3 4 5	
		s- r-					0123	012345	g p	012345	012345	F S B V O				S F L							1 2 3 4 5	
		s- r-					0123	012345	g p	012345	012345	F S B V O				S F L							1 2 3 4 5	
		s- r-					0123	012345	g p	012345	012345	F S B V O				S F L							1 2 3 4 5	
		s- r-					0123	012345	g p	012345	012345	F S B V O				S F L							1 2 3 4 5	
		s- r-					0123	012345	g p	012345	012345	F S B V O				S F L							1 2 3 4 5	
		s- r-					0123	012345	g p	012345	012345	F S B V O				S F L							1 2 3 4 5	
		s- r-					0123	012345	g p	012345	012345	F S B V O				S F L							1 2 3 4 5	
		s- r-					0123	012345	g p	012345	012345	F S B V O				S F L							1 2 3 4 5	
		s- r-					0123	012345	g p	012345	012345	F S B V O				S F L							1 2 3 4 5	
		s- r-					0123	012345	g p	012345	012345	F S B V O				S F L							1 2 3 4 5	
		s- r-					0123	012345	g p	012345	012345	F S B V O				S F L							1 2 3 4 5	
		s- r-					0123	012345	g p	012345	012345	F S B V O				S F L							1 2 3 4 5	
		s- r-					0123	012345	g p	012345	012345	F S B V O				S F L							1 2 3 4 5	
		s- r-					0123	012345	g p	012345	012345	F S B V O				S F L							1 2 3 4 5	
		s- r-					0123	012345	g p	012345	012345	F S B V O				S F L							1 2 3 4 5	

Cracks <2 cm: Evidence of microcracks <2 cm long. 0 = 0; 1 = <1/dm^2; 2 = 1-5/dm^2; 3 =5-10/dm^2; 4=≥10/dm^2

GD & Pit: G = positive **e**vidence of granular disentigration (loose grains) **P** = pitting evident

Crack Length defined as total exposed length of the crack; equivalent to a surface exposure length NOT a 'caliper' length.

Fabric type: f=foliation; **s**=fossils; **b**=bedding; **v** = vein or dyke **o**=other

Lichen&varnish: 0 = 0%, 1=>0and<10; 2=>10 and<30; 3=>30 and<60; 4 = >60 and <90; 5 =>90

Avg. Grain Size = representative size of grains throughout the boulder

Parallel: S = surface, F = fabric, L = long axis of clast or outcrop

Sheet Ht = the height of the spall or exfolation resulting from a surface-parallel crack; n/a for other cracks

Crack Parallel to: S: Surface, F: Fabric (joints, bedding); L = long axis

weathering Index:
0 = no crack (step)
1: fresh with evidence of recent rupture (flakes/pieces)
2: sharp, no rounded edges anywhere
3: mostly sharp with occasional rounded edges
4: mostly rounded edges with occasional sharp
5: all rounded edges
NOTE: 0, or 1 must have clear evidence of a recent break: i.e. small pieces left

Exposure
use angle of the boulder at the ground
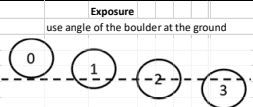
**Feature (crack, fossil, pore)
Size Classes (mm)**

VC = Very Coarse (>20)
C = Coarse (<10 and >5)
M = Medium (<5 and >2)
F = Fine (<2 and >1)
VF = Very Fine (<1)

Quantity Classes

'1' - Few: < 1 per area
'2' - Common: 1-5 per area
'3' - Very common: > 5 and < 10 per area
'4' - Many: ≥ 10 per area

10 cm x 10 cm

VC use
100 cm x 100 cm
(not shown)

VC >

M & C use
10cm x 10 cm

>C > ●
5mm

20mm

20mm

● **>M >** •
5mm   2mm

• **> F >** :
2mm   1mm

F & VF use
1cm x 1cm

1 cm x 1 cm

: **> VF**
1mm

0   1   2   3   4
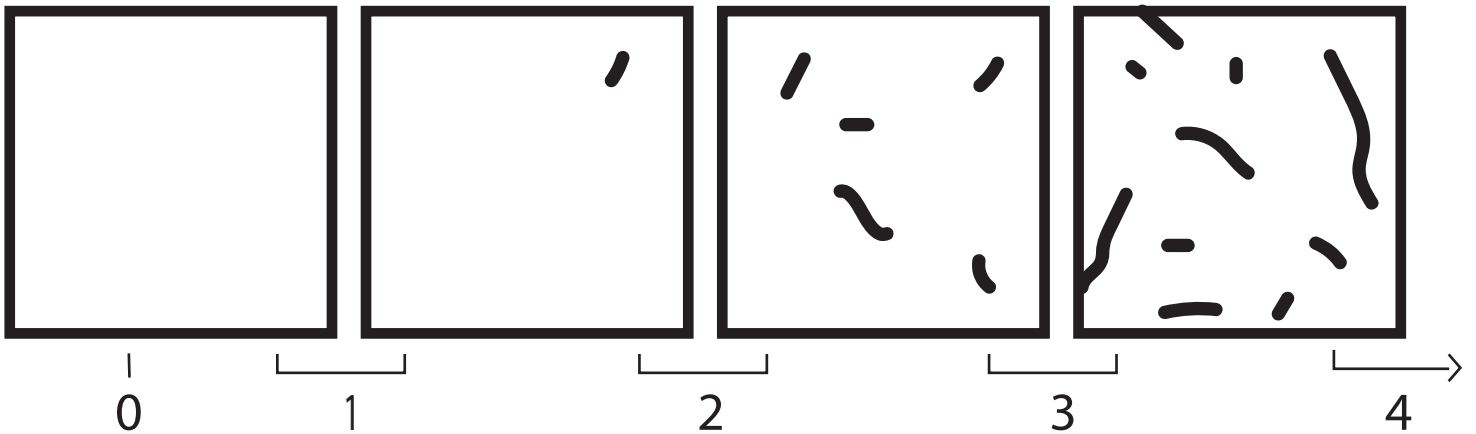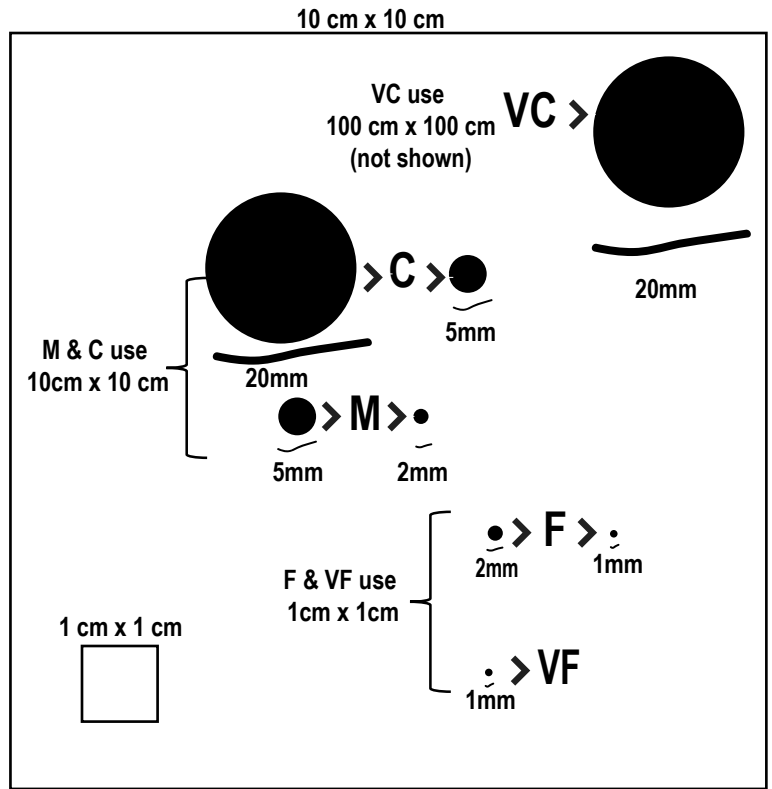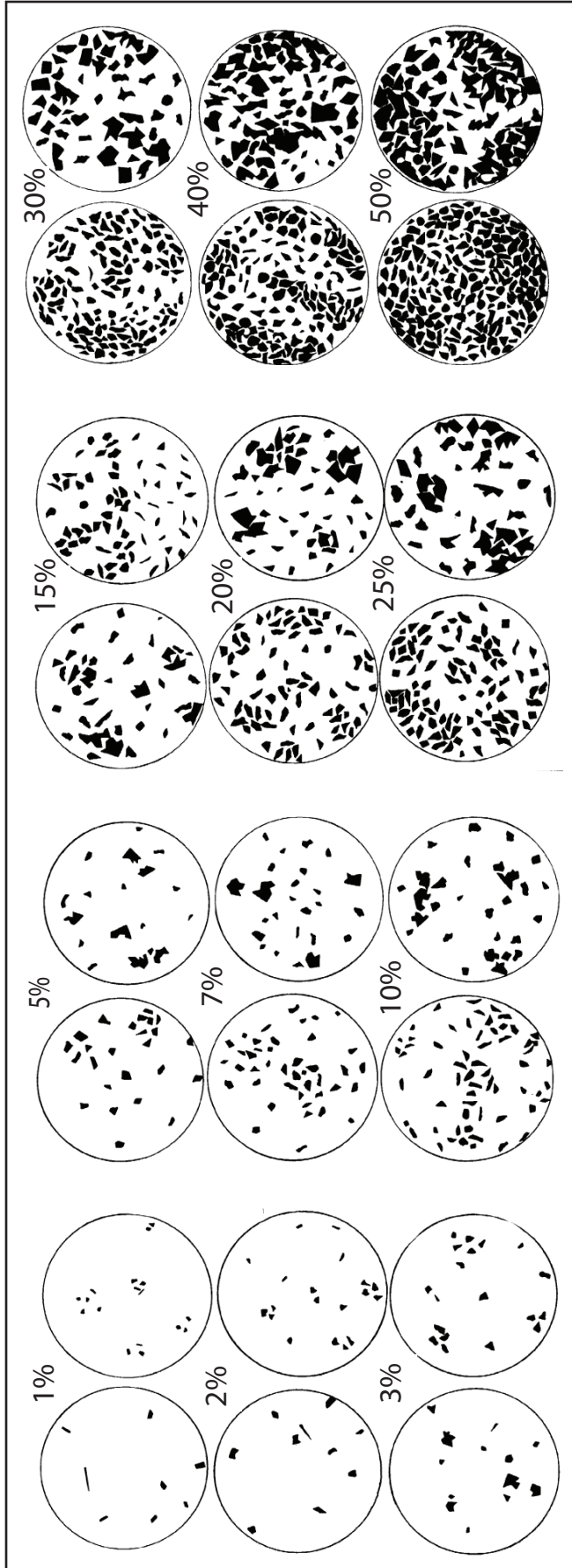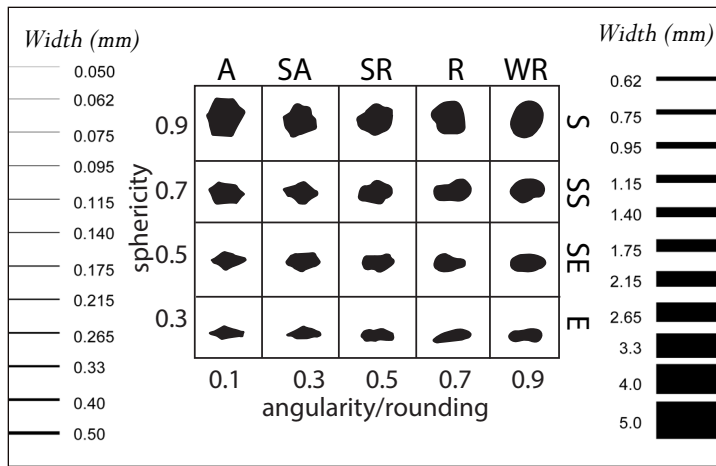
FIGURE 6

FIGURE 7

note to copy-editor: this figure should be published to scale when the document is viewed at 100%

FIGURE 8

FIGURE 9

FIGURE 10